Andean Geology 39 (1): 133-157. January, 2012

Andean Geology
formerly Revista Geológica de Chile
www.andeangeology.cl

Tectonostratigraphic analysis of the Late Triassic-Early Jurassic syn-rift sequence of the Neuquén Basin in the Sañicó depocentre, Neuquén Province, Argentina

Leandro D'Elia[1], Martin Muravchik[2], Juan R. Franzese[1], Luciano López[3]

[1] *Centro de Investigaciones Geológicas (CIG), Universidad Nacional de La Plata-CONICET, Calle 1 No. 644 B1900TAC, La Plata, Argentina.*
ldelia@cig.museo.unlp.edu.ar; franzese@cig.museo.unlp.edu.ar

[2] *Department of Earth Science, University of Bergen, Allégaten 41, N-5007, Bergen, Norway.*
martin.muravchik@geo.uib.no

[3] *Instituto de Recursos Minerales (INREMI), Universidad Nacional de La Plata-CONICET, Calle 1 No. 644 B1900TAC, La Plata, Argentina.*
lopezluciano@hotmail.com

ABSTRAc T. The initial syn-rift infill (Upper Triassic-Lower Jurassic) of the Neuquén Basin involved a complex stacking of lava, pyroclastic and sedimentary units, in which volcanic rocks compose up to 72% of the infill. The high-quality outcrops of the southern Sañicó depocentre, which was uplifted and exposed during the Andean orogeny, were studied in order to determine the lithofacies arrangements, the tectonostratigraphic framework and the main controls over the syn-rift succession. The tectonostratigraphic study made it possible to determine three sections characterized by the predominance of effusive, pyroclastic or sedimentary deposits. These sections indicate three different evolutionary stages of the volcanic rifting. The onset of this rift stage was dominated by effusive rocks with minor ignimbrite and alluvial volcaniclastic units, which indicates the occurrence of composite volcanoes at the boundaries of the depocentre. The mid-rift stage was characterized by the development of fault-controlled, large ignimbrite deposits intebedded with volcaniclastic alluvial deposits and lava units, which suggests a volcano-tectonic depression related to asymmetrical and incremental subsidence. The end of the volcanic rifting event was marked by a decrease in the volume of the volcanic rocks and the occurrence of low-relief effusive aggradational volcanic edifices and lava fields in close relation with alluvial, deltaic and lacustrine units. The analysis of the syn-rift sequence in the Sañicó depocentre showed the complex relationships between tectonic and volcanic controls which occurred in different magnitudes and times during the rifting evolution.

Keywords: Neuquén Basin, Argentina, Syn-rift, Tectonostratigraphy, Volcanism and sedimentation.

RESu MEN. Análisis tectonoestratigráfico de la secuencia de sin-rift Triásico Superior-Jurásico Inferior de la c uenca Neuquina en el depocentro de Sañicó, provincia del Neuquén, Argentina. Los depósitos de sin-rift desarrollados durante la etapa de 'rifting' inicial (Triásico Superior-Jurásico Inferior) de la Cuenca Neuquina están constituidos por un arreglo complejo de unidades lávicas, piroclásticas y sedimentarias, donde las rocas volcánicas componen hasta un 72% del relleno. La inversión andina causó la exhumación y la excelente exposición de las rocas que componen este ciclo en el depocentro de Sañicó, ubicado en el límite sur de la Cuenca Neuquina. El objetivo del presente trabajo es el estudio del relleno sin-tectónico inicial, poniendo especial énfasis en los arreglos de facies, el marco tectonoestratigráfico y los principales controles que operaron durante la evolución del relleno inicial de la cuenca en este depocentro. El análisis estratigráfico y de facies reveló la distribución lateral y vertical de las unidades involucradas en el relleno, mientras que el estudio tectonoestratigráfico permitió la subdivisión del relleno en tres secciones, caracterizadas por la predominancia de rocas volcánicas efusivas, rocas piroclásticas o sedimentarias, las que a su vez marcan tres estadios evolutivos para la secuencia de sin-rift. El inicio de la secuencia de rift estuvo dominado por rocas efusivas con menor participación de ignimbritas y unidades aluviales volcaniclásticas que fueron interpretadas como representantes de volcanes compuestos ubicados en posición de borde del depocentro. La etapa intermedia estuvo caracterizada por extensos y potentes depósitos de ignimbritas controlados por fallas que se intercalan con sucesiones aluviales y lavas. Estas unidades permitieron determinar depresiones volcano-tectónicas relacionadas a una subsidencia asimétrica e incremental. La finalización de la etapa de 'rifting' volcánico en este depocentro se caracterizó por una disminución de la actividad volcánica representada por aparatos volcánicos agradacionales de bajo relieve y campos de lava asociados con unidades aluviales, deltaicas y lacustres. El análisis de la secuencia de sin-rift en el depocentro de Sañicó manifiesta la relación compleja que existe entre los controles tectónicos y volcánicos, que se presentaron con diferentes magnitudes y en diferentes momentos durante la evolución del 'rifting'.

Palabras clave: Cuenca Neuquina, Argentina, Sin-rift, Tectonoestratigrafía, Volcanismo y sedimentación.

1. Introduction

The Neuquén Basin is located in the Andean margin between 32 and 40°S latitude (Fig. 1). It constitutes one of the most distinctive features which originated during the Upper Triassic-Lower Jurassic on the western edge of Gondwana by continental extension. Syn-rift depocentres were developed during the initial stages of the basin as isolated troughs following a multi-directional pattern, linked with profuse magmatic activity (Legarreta and Uliana, 1996; Franzese and Spalletti, 2001; Howell *et al*., 2005). The initial depocentres, characterized as a series of long, narrow half-grabens, were filled by a complex array of volcanic and volcaniclastic materials which are known as the Precuyano Cycle (Gulisano *et al*., 1984). In particular, it is important to highlight the huge volumes of lava flows and pyroclastic materials that constitute the syn-rift sequence and their strong imprint on the sedimentary systems. Although there have been a number of contributions on the evolution and fill of the basin (Howell *et al*., 2005, and papers therein), studies of the early depocentres of the Neuquén Basin have concentrated on either stratigraphic analyses (Gulisano, 1981; Gulisano and Pando, 1981; Gulisano *et al*., 1984; Riccardi and Gulisano, 1990; Leanza, 1990; Gulisano and Gutiérrez Plieming, 1994; Llambías *et al*., 2007; Schiuma and Llambías, 2008) or on tectonostratigraphic analyses, instead of focusing on the occurrence of extension and volcanism, and the relationships between the latter and its imprint over sedimentary environments (Álvarez and Ramos, 1999; Franzese *et al*., 2006; Franzese *et al*., 2007; Muravchik *et al*., 2008; Giambiagi *et al*., 2008a; Giambiagi *et al*., 2008b; Giambiagi *et al*., 2008c; Pángaro *et al*., 2009). The southern part of the Neuquén Basin is characterized by reactivated normal faults and reverse faults related to the evolution of the Andean chain that led to well-exposed Mesozoic successions of the initial stage of the basin. The aims of this study are to carry out a tectonostratigraphic analysis of the volcanic syn-rift deposits cropping out in the Sañicó depocentre -to the south of the Neuquén Province, Argentina- focusing both on the depositional processes and on the relationship between tectonic and volcanic controls in the development of the sedimentary sequence, and to devise an evolution scheme of the depocentre. The study of the syn-rift succession was carried out through detailed geological mapping and measuring of stratigraphic and sedimentary logs. Petrographic analyses were made to establish the compositional characteristics of lava and pyroclastic rocks and the nature of the provenance of the sedimentary facies.

2. Geological Setting

The Neuquén Basin is located on the eastern side of the Andes in central Argentina, and it constitutes one of the most important hydrocarbon basins in South America. It is limited by a volcanic arc to the west and by two mesocratonic areas, the Sierra Pintada System and the North Patagonian Massif, to the north-east and south-east respectively (Fig. 1). The basin has a multiphase tectonic history involving an early stage of extension (Upper Triassic-Lower Jurassic) followed by a post-rift phase superimposed with the development of the magmatic arc (Ramos and Folguera, 2005; Ramos, 2009). Subsequent stages of inversion and extension, which occurred during Mesozoic and Cenozoic times, relate to the evolution of the Andean orogeny (Vergani *et al*., 1995; Ramos and Folguera, 2005; Howell *et al*., 2005; Cristallini *et al*., 2006; Mpodozis and Ramos, 2008). The basin recorded at least two episodes of rift during its origin. In the first syn-rift stage (Rhaetian-Pliensbachian) the initial configuration of the basin was characterized by the development of isolated deep depressions bounded by normal faults and filled with volcano-sedimentary successions (Franzese and Spalletti, 2001). Subsurface studies show them as a series of half-grabens with variable polarity, intersected by *en-echelon* transfer faults (Vergani *et al*., 1995; Cristallini *et al*., 2006). The stratigraphy of the initial syn-rift of the basin is complex, involving a continental volcano-sedimentary succession known as the Precuyano Cycle (Gulisano *et al*., 1984; Gulisano, 1993), which is constituted by different lithostratigraphic units (Franzese and Spalletti, 2001). The second stage of rifting (Pliensbachian-Toarcian) involved mainly marine deposits known as the Cuyano Cycle, which overlapped with the onset of the transition to the post-rift stage (Vergani *et al*., 1995).

FIG. 1. Distribution of rift depocentres in the Neuquén Basin, Argentina, and in the Coastal Cordillera, Chile. Location of the study area is highlighted in a black square. Modified from Franzese and Spalletti (2001).

During the Andean orogenic cycle, different deformation periods caused the inversion and uplifting of the basin, initially during the Late Jurassic and subsequently since the Late Cretaceous (Howell *et al*., 2005; Ramos and Folguera, 2005; Morabito *et al*., 2011). The southern part of the basin records the typical areas which have usually been taken as a case study for the analysis of the initial syn-rift of the basin (Gulisano and Pando, 1981; Leanza, 1990; D'Elia and Franzese, 2005; Muravchik and Franzese, 2005; Franzese *et al*., 2006; Franzese *et al*., 2007; D'Elia, 2008; Muravchik *et al*., 2008; Bilmes *et al*., 2008; Spalletti *et al*., 2010; D'Elia, 2010; Muravchik and D'Elia, 2010; Muravchik *et al*., 2011; D'Elia *et al*., 2012). The study area is located on the southern boundary of the Neuquén Basin, in the limit between the Neuquén and Río Negro provinces, Patagonia, Argentina (Fig. 1). In this area, the initial depocentres have recently been redefined, among them the Sañicó depocentre (Muravchik *et al*., 2008; D'Elia, 2010; D'Elia *et al*., 2012). Reactivated normal faults and reverse faults led to well-developed successions of the basin (Fig. 2A, C), which were correlated by different authors with pre-rift, syn-rift and transitional syn-rift to post-rift units (Fig. 2B; Franzese and Spalletti, 2001; Muravchik *et al*., 2008). Locally, Cenozoic volcanic and sedimentary rocks overlie the initial fill of the basin.

Pre-rift units are constituted by metamorphic and igneous rocks (Cushamen Formation, Volkheimer, 1964; Mamil Choique Formation, Sesana, 1968) of Upper Paleozoic age (Varela *et al*., 2005).

The syn-rift fill lies unconformably over the pre-rift units. It is constituted by the Sañicó For-

mation (Fig. 2C; Stipanicic, 1967; Stipanicic *et al*., 1968). It is important to point out that some authors include the siliciclastic deposits of the Upper Triassic Paso Flores Formation (Frenguelli, 1948; Morel and Ganuza, 2002), that crops out in the vicinities of the study area, to the Precuyano Cycle (Franzese and Spalletti, 2001). Nevertheless, most of the Paso Flores Formation lies outside of the Sañicó Depocentre. The significant hiatus between this unit and the Sañicó Formation and the strong difference in lateral and vertical distribution of the two units suggest that the Paso Flores Formation should not be incorporated to the syn-rift evolution of the Sañicó Depocentre (Fig. 2). Therefore, in this paper we will concentrate in the analysis of the Sañicó Formation. The Sañicó Formation is composed by lava, pyroclastic and siliciclastic deposits (Lambert and Galli, 1950; Galli, 1953; Galli, 1969) constrained to a Hettangian-Sinemurian age on the basis of stratigraphic analysis (Stipanicic, 1967; Stipanicic *et al*., 1968). Recent data taken from the underlying Piedra del Águila Formation close to the study area, constrained this unit to the Sinemurian (Spalletti *et al*., 2010).

The transitional syn-rift to post-rift deposits unconformably overlies both basement and syn-rift

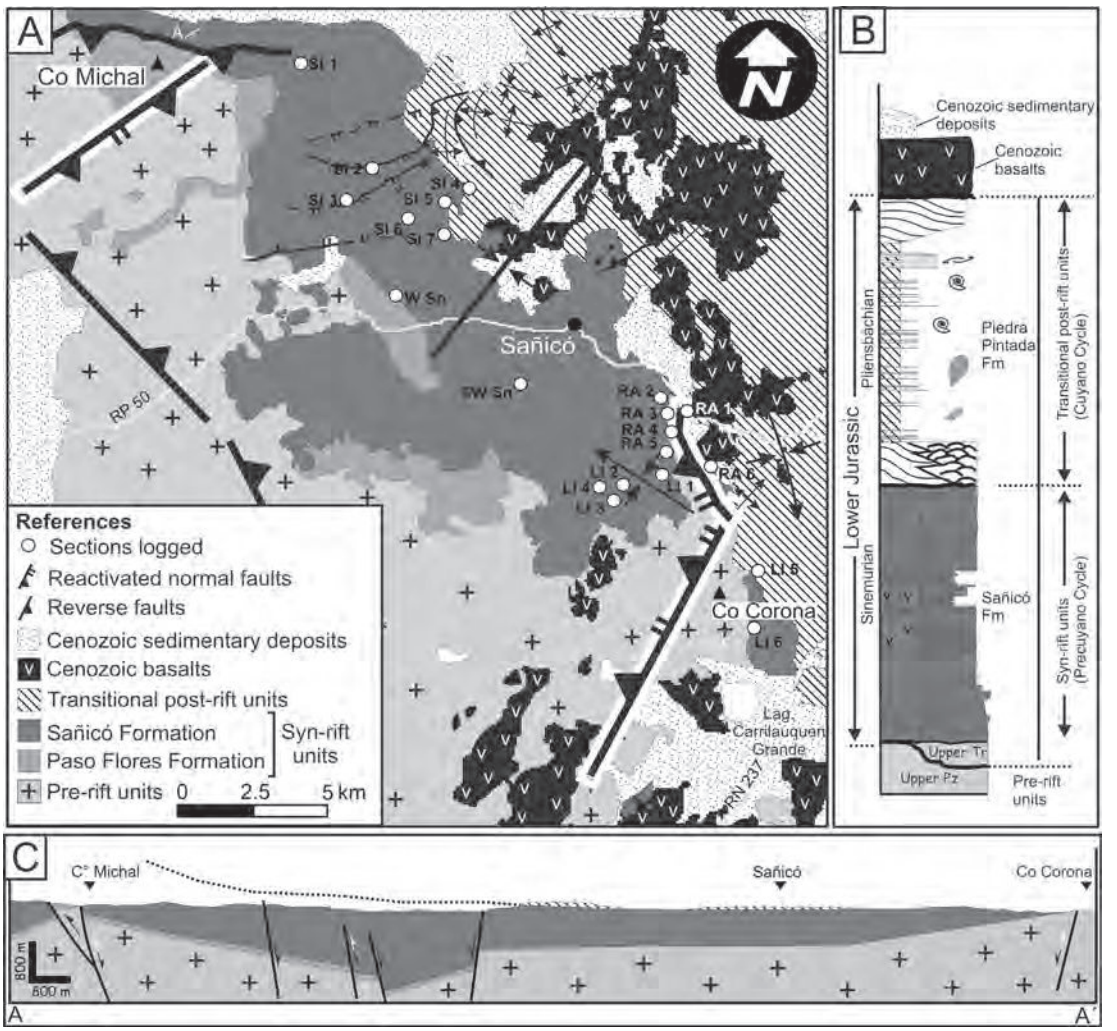

FIG. 2. Geological maps of the study area and location of logged sections. **A.** Geological map of the Sañicó depocentre and location of logged sections; **B.** Schematic stratigraphic column representing the different units present at the Sañicó area; **c .** Cross-section of the Sañicó depocentre.

units (Fig. 2A) across a major discontinuity that is related to the widespread marine transgression of the Neuquén Basin (Gulisano *et al*., 1984). These deposits were grouped into the Piedra Pintada Formation, which is composed of coeval siliciclastic and carbonate deposits (Fig. 2B; Herbst, 1966; Stipanicic *et al*., 1968; Stipanicic, 1969) of Pliensbachian age (Damborenea *et al*., 1975; Damborenea and Manceñido, 1993), which were interpreted as shallow-marine siliciclastic and carbonate deposits that change laterally and upward into off-shore deposits (Gulisano and Pando, 1981; Gulisano *et al*., 1984).

3. The Sañicó depocentre

The tectonostratigraphic framework of the Sañicó depocentre was established on the basis of structural and geological mapping, as well as on the sections logged (Figs. 2A; 7A and 8B). It was mainly filled by a volcano-sedimentary continental succession (the Sañicó Formation), and secondarily by marine deposits of the Cuyano Cycle (Fig. 2A, C). The faulted margins of the Sañicó depocentre are constituted at present by high degree to partially inverted fault systems (*i.e*., the Cerro Michal and the Cerro Corona fault systems. Both boundaries of the depocentre are shown as thick-skinned emergent anticlines forming NE-oriented folds with minor ENE- and NNW-trending structures (Fig. 2A, C). Within the depocentre, minor partially reactivated normal faults parallel and oblique to the margin structures were registered (Fig. 2A). Several features may be considered as indicators of fault reactivation and inversion which are mainly related to abrupt changes in topography and stratigraphy associated with the major tectonic boundaries. The Cerro Michal fault system (Fig. 2A, C) separates the syn-rift succession in a thin sequence of lava flows to the NW of the faults from a thick syn-rift succession with more than a thousand metres of lava, pyroclastic and sedimentary rocks to the SE (Fig. 7A). To the SE of the Cerro Michal fault system, the syn-rift fill of the depocentre constitutes a large syncline which can be traced for 25 km to the Cerro Corona fault system, where the syn-rift succession is absent or reaches its minimum thickness (Figs. 2A, 2C and 7A). This suggests that the Cerro Michal and Cerro Corona fault systems acted as the boundaries of the depocentre. Reverse faults located on the western side of the study area caused the regional tilting of the syn-rift sequence to the east. Perpendicular to the bounding fault systems the syn-rift fill may be followed for approximately 5 km (Fig. 2A). Beyond this point it is unconformably covered by deposits corresponding to the Cuyano Cycle. Although the Sañicó depocentre was affected by the Andean deformation, the geometries and dimensions recognized herein are comparable with those of the syn-rift depocentres documented in subsurface (Vergani *et al*., 1995; Cristallini *et al*., 2006; Pángaro *et al*., 2009).

4. Stratigraphy of the Sañicó depocentre

According to the different rock-forming and fragment-forming processes, three major groups of facies were distinguished: lava, pyroclastic and sedimentary. The first two are associated with primary volcanic processes, while the latter is related to secondary surface processes (*i.e*., resedimentation, reworking, weathering, mass wasting and erosion). In order to avoid the possible descriptive and genetic imbalances that frequently exist between volcano-related, pyroclastic-related and sedimentary-related facies, in this work a non-genetic descriptive scheme is adopted to describe the facies (McPhie *et al*., 1993; Branney and Kokelaar, 2002; Walker, 2006, respectively). Subsequently, each facies was interpreted in terms of its rheological and hydrodynamic conditions (Fig. 3).

4.1. Lava lithofacies

They constitute up to 38% of the total thickness of the volcanic syn-rift succession. Five lithofacies have been defined according to their composition, on the basis of phenocryst assemblages, and their internal structures (Fig. 3). The coherent andesite lithofacies *(cA;* Fig. 4A, B*)* and brecciated andesite lithofacies *(brA;* Fig. 4C, D) constitute the most abundant lava lithofacies of the syn-rift fill (Figs. 3, 7A and 8A), while the acid lava facies (coherent dacite lithofacies; *cD* and coherent and brecciated rhyodacite and rhyolite lithofacies; *cRD, cR, brRD, brR;* Figs. 3 and 4F-G) are poorly represented in the syn-rift sequence (Figs. 7A and 8A).

The lava facies of the syn-rift sequence reveal a multi-compositional trend with predominance of andesite lithofacies. The range of textural arrangements and differences in phenocryst abundance indicate

Code	Lithology	Structures and textures	Geometry and thickness	Interpretation
Lava				
cA	Andesite	Coherent porphiritic lava, massive and non-vesiculated, columnar joints	Tabular (concordant or discordant) or dome-shaped, > 2 m thick. Superimposed events form succesion of dm	Intermediate lava flows, lava domes and dikes
brA	Andesite	Brecciated, jigsaw-fit or clast-rotated textures, non-graded, poorly sorted, clast-supported with minor matrix breccias, massive or stratified tabular		
cD, cRD and cR	Dacite, Rhyodacite and rhyolite	Coherent, massive or flow banded, non-vesiculated, porphyritic, aphanitic or seriate lavas. In some case the groundmas presents micropoikilitic texture and pervasive silicification	Dome-shaped, irregular, concordant or discordant, > 5 m thick, related with faults, slightly extended laterally	Acid lava domes and necks and to a lesser extent lava flows
brRD and brR	Brecciated rhyodacite and rhyolite	Brecciated, jigsaw-fit textures, non-graded, poorly sorted, clast-supported in which clasts are generally 10 – 0.5 m, often pervasive silicification		
Pyroclastic				
mBr (i)	Breccia	Massive monomictic breccia, non-graded to inverse-graded, poorly sorted, clast-supported. Juvenile pyroclasts are non to poorly vesiculated andesitic porphyritic glassy clasts	Tabular, 2–5 m thick.	Block and ash, short-lived pyroclastic flow deposits
mlBr and dslBr	Breccia	Massive or stratified, heterolithic, non-graded, poorly to moderately sorted, matrix-supported or clast-supported, fine and pumiceous-rich medium breccias (clasts up to 1 m)	Lenses, irregular-shaped or tabular, up to 3 m thick	Rapid progressive aggradation from fluid escape-dominated to grain flow-dominated depositional flow boundary of a PDC
mLT (e;i;pip)	Lapilli-tuff	Massive or oriented fabrics defined by planar or linear arrangements of lapilli, isotropic (i), fines-poor pipes (pip), rarely eutaxitic texture (e), poorly to moderately sorted	Tabular cm–m thick or amalgamated in sequences of hundred m thick	Rapid aggradation from high-concentration fluid escape-dominated (with or without a component of granular flow) depositional flow boundary of a PDC
dsLT	Lapilli-tuff	Diffuse-stratified, non-graded to graded, poorly to moderately sorted	Tabular or lenticular, cm–dm thick	Granular flow-dominated boundary of a PDC
//sT and xsT	Lapilli-tuff	Stratified and cross bedded, well sorted to moderately sorted, fine tuff to lapilli-tuff	Tabular or lenticular, cm–dm thick	Traction-dominated flow boundaries of a PDC
mpL	Lapillistone	Massive, well to moderately sorted clast-supported (angular pumice lapilli with subordinate lithic lapilli and ash)	Tabular or irregular, cm thick	Proximal deposits by fallout from eruption plumes
sT	Tuff	Thin stratified, laminated or massive, well-sorted fine tuff	Tabular, cm thick	Distal fall deposits from eruption plumes or from ash-rich PDC
Sedimentary				
Brmm	Breccia	Massive, unsorted, matrix-supported to clast-supported, monomictic, megabreccias (clasts μ–50 cm, megablocks up to 20 m with jigsaw-fit to clast-rotated textures)	Irregular bodies extended laterally several decametres thick	Volcanic debris avalanche flow deposits
Brm	Pumice breccia	Massive, graded, clast-supported, polymodal matrix, fine-grained pumiceous breccias	Tabular, 5–30 cm thick	Corse-grained hyperconcentrated sheet flow deposits
Gmm	Conglomerate	Massive, monomictic or polymictic, poorly sorted, sandy matrix-supported, medium- to coarse-grained conglomerates	Lobate or tabular, 2–5 m thick	Non cohesive debris flow deposits
Gm	Conglomerate	Massive, pebbles oriented with their long axes parallel to stratification, poorly sorted clast-supported, polymodal matrix, monomictic or polymictic, fine- to medium- grained conglomerates	Tabular cm–2 m thick	Corse-grained hyperconcentrated sheet flow deposits
Gp(a)	Conglomerate	Planar cross stratified with imbricate fabric, clast-supported, moderately sorted, fine-grained conglomerates	Lenticular, 0,5–1 m thick	Bedload transport and deposition from stream flows
Gp(b)	Conglomerate	Large-scale cross stratified clast-supported, poorly sorted, clast-supported, polymodal matrix, polymictic, fine- to medium-grained conglomerates	Large-scale foresets, 2–3 m thick	Coarse-grained hyperconcentrated flow deposits in large-scale planar cross surfaces
SGh / Sh(a)	Pebbly sandstone / sandstone	Horizontally laminated or stratified, normal grading, moderately sorted	Tabular, 5–20 cm thick	Sandy hyperconcentrated sheet flow deposits
Sx	Sandstone	Trough or planar cross-bedded, coarse-grained, moderately- to well-sorted	Lenticular or tabular, up to 1 m thick	Bedload transport and deposition from stream flows
Sh(b)	Sandstone	Horizontally laminated, medium-grained, to well-sorted	Tabular, up to 20 cm thick	Sheet flood deposits in upper-flow regime conditions
Sm	Tuffaceous sandstones	Massive, moderately sorted with scattered pumice lapillus	Tabular, 10–30 cm thick	Sandy hyperconcentrated sheet flow deposits
Fl	Siltstone	Massive or horizontal lamination	Laminar, 1–3 cm thick	Settling from suspensions in low energy water bodies
Ll(a)	Limestone	Horizontally laminated limestones mudstone, highly silicified	Irregular, 5–20 cm thick	Non marine carbonate precipitation
Ll(b)	Limestone	Microbial laminated or undulatory laminated boundstones	Irregular, 5–20 cm thick	Stromatolic deposits

FIG. 3. Facies description and interpretation. The codes for lava facies were created for this work. The codes for pyroclastic facies (PDC=Pyroclastic Density Currents) were taken from Branney and Kokelaar (2002), while the codes for sedimentary facies were modified from Miall (1978) and Smith (1986).

polygenetic textures, suggesting a two-stage cooling history (*i.e*., in the magma chamber or near surface and surface conditions) and complex feeder systems (Wilson, 1989; Marsh, 2000; Best and Christiansen, 2001). The holocrystaline to porphyritic glassy texture indicated by spherulites (high temperature devitrification of glass) suggests that liquids cooled below their normal point of crystallization or supercooled (McArthur *et al*., 1998; Best and Christiansen, 2001). Most of the structural patterns imply that lava facies were deposited as subaerial or free-water shallow intrusion, although in some cases hyaloclastic structures suggest damp conditions (McPhie *et al*., 1993). The coherent facies involve areas of slow cooling or gentle shear rate (Kilburn, 2000; Stewart and McPhie, 2003). By contrast, the occurrence of jigsaw breccias implies that the brecciation was developed by brittle fractures which occurred in response to contraction during the cooling, whereas the stratified autobreccias with rotated clasts, suggest that the main fragmentation mechanism was brittle fracture in response to transport (McPhie *et al*., 1993; Stewart and McPhie, 2003; Stewart and McPhie, 2006). On the basis of textural, structural and geometrical parameters different volcanic bodies may be defined, such as andesitic lava flows, lava domes and dikes composed of coherent or both coherent and brecciated lava facies (Figs. 3 and 4A-D); dacitic and rhyodacitic necks and lava domes generally constituted by coherent facies (Figs. 3 and 4E-G); and rhoylitic lava flows formed by coherent or autobrecciated facies (Cas and Wright, 1987; McPhie *et al*., 1993; Németh and Ulrike, 2007).

4.2. Pyroclastic lithofacies

They are the second most important lithology and constitute up to 34% of the volcanic syn-rift succession (Figs. 7A and 8A). Seven lithofacies have been defined (Fig. 3) according to combinations of texture, structure and composition determined on the basis of cognate crystal fragments. Except the massive lithic breccia lithofacies, which presents an andesitic composition, the rest of the lithofacies have a dacitic to rhyodacitic composition with minor amounts of rhyolites. Evidence of high temperature welding (*i.e*., welded shards, matrix spherulites, rheomorphic deformation) is generally absent. In most of the cases the pyroclastic facies show a low-grade of welding and diagenetic alteration, vapour phase crystallization or silicification. The pyroclastic facies of the volcanic syn-rift succession show different eruptive mechanisms, as well as different processes of transport and deposition. The occurrence of non- to poorly vesiculated porphyritic glassy juvenile clasts with an andesitic composition in the massive breccia facies *(mBr;* Fig. 5A*)* suggests that this was originated by gravitational collapse of lava flows or lava domes, causing short-lived pyroclastic flows, which formed block and ash flow deposits (Cas and Wright, 1987; McPhie *et al.*, 1993). Pumiceous lapilli and cuspate shards in acid pyroclastic deposits indicate that they were caused by a magmatic eruption with an effective degree of fragmentation (Cas and Wright, 1987). Most of the acid pyroclastic facies (*mlBr*, *mLT*, *dsLT*, *//sT* and *xsT*; Fig. 3) were formed by progressive aggradation near the lower depositional flow boundary of a pyroclastic density current (PDC) (Branney and Kokelaar, 2002), whereas the *pmL* and *sT* facies were deposited by fallout from eruption plumes, forming fall layers. The massive and diffuse-stratified lithic breccia facies (*mlBr-dslBr;* Fig. 5B) may be interpreted as a coarse facies of ignimbrite, deposited through the lower flow boundary of a PDC in which turbulence and traction were suppressed (Branney and Kokelaar, 2002). The absence of tractional structures or diffusive stratification with linear fabric indicates rapid progressive aggradation from the fluid escape-dominated to grain flow-dominated depositional flow boundary of a PDC (Branney and Kokelaar, 2002; Kokelaar *et al*., 2007). The massive lapilli-tuff facies (*mLT;* Fig. 5C, D) indicates rapid aggradation from the high-concentration fluid escape-dominated depositional flow boundary of a PDC, whereas the massive lapilli-tuff facies with a directional fabric *(mLTf)* records deposition from a flow-boundary zone dominated by fluid escape processes, but with a component of granular flow (Branney and Kokelaar, 2002). In this case study the massive lapilli-tuff facies with eutaxitic fabric *(emLT)* commonly represents cold-burial compaction associated with diagenesis (McPhie *et al*., 1993; Gifkins *et al*., 2005) and minority welding deformation during post-emplacement stages (McArthur *et al*., 1998). The diffuse-stratified lapilli-tuff facies (*dsLT;* Fig. 5E) is deposited when flow-boundary zone conditions are intermediate between a fluid escape-dominated and a traction-dominated flow-boundary zone, causing the granular flow-dominated boundary of a PDC (Branney and Kokelaar, 2002; Brown *et al*., 2007;

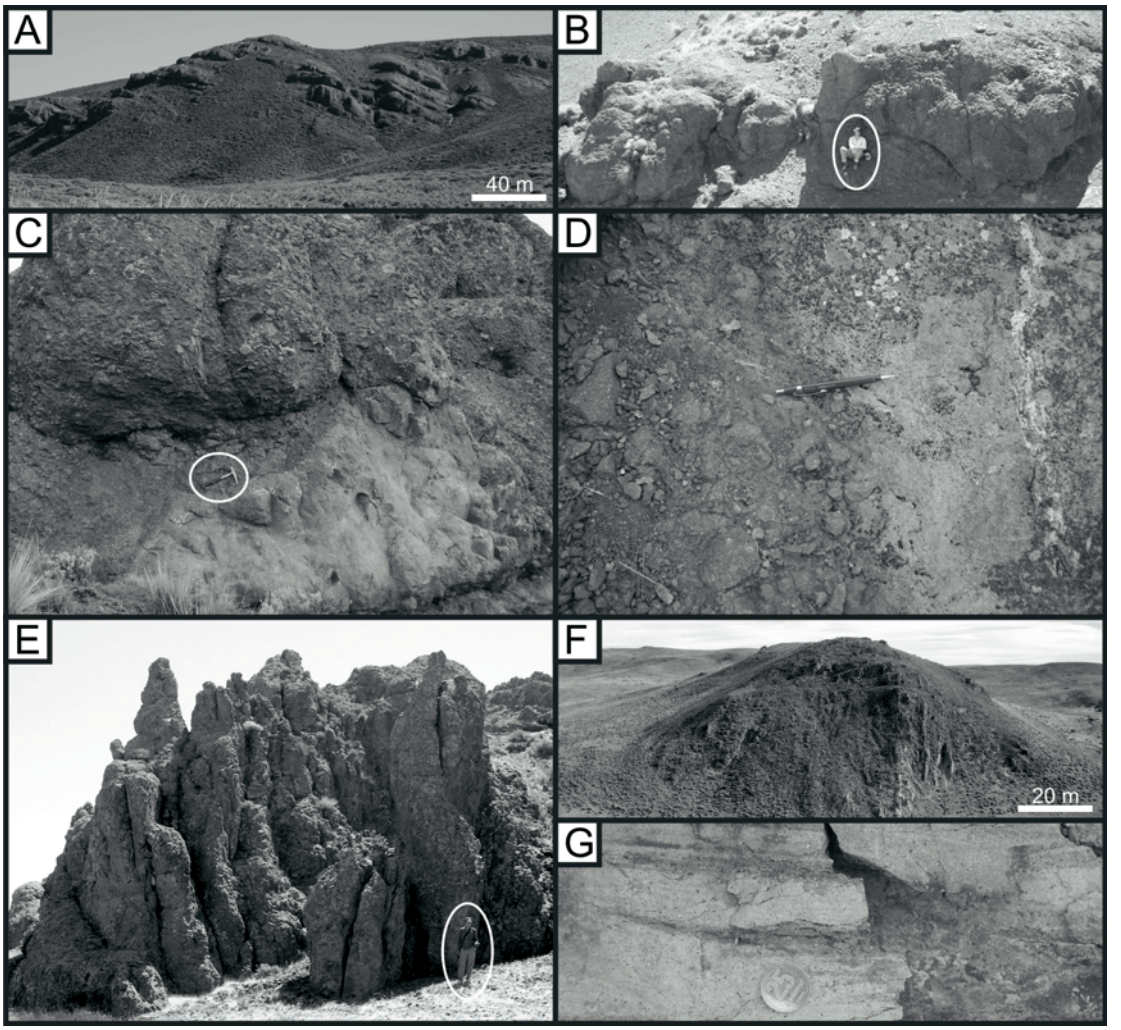

FIG. 4. Lava facies. **A.** Outcrop-scale photograph of the andesitic lava flow succession; **B.** Brecciated andesitic facies (*brA*) formed a small lava dome (circle indicates person for scale); **c .** Coherent and brecciated andesitic facies (*cA, brA*) involved in lava flows (circle indicates a hammer for scale); **D.** Outcrop photograph showing transitional contact between coherent and brecciated andesitic facies; **E.** Dacitic lava facies developed a neck body (circle indicates person for scale); **F.** Coherent rhyodacitic lava facies formed a criptodome (*cRD*); **G.** Detail of coherent rhyodacitic lava facies (*cRD*).

Kokelaar *et al*., 2007). Stratified and cross bedded tuff facies *(//sT, xsT;* Fig. 5*)* indicate deposition from the traction-dominated flow boundaries of a PDC (Branney and Kokelaar, 2002). The massive pumice lapillistone facies *(pmL;* Fig. 5G*)* is interpreted as proximal deposits by fallout from eruption plumes. The presence of pumice fall layers within a sheet of *mLT* records temporary cessations of flow (*i.e.*, Plinian or sub-Plinian pumice fall units) (Cas and Wright, 1987). The thin stratified, laminated or masive tuff facies *(sT)* includes distal fall deposits from eruption plumes or from ash-rich pyroclastic density currents (Cas and Wright, 1987; Branney and Kokelaar, 2002).

4.3. Sedimentary lithofacies

The sedimentary facies constitute up to 28% of the volcanic syn-rift succession and are composed by siliciclastic and carbonate rocks. Clastic sedimentary facies (volcano-related and non-volcano-related) were considered as epiclastic facies (*sensu* Cas and Wright, 1987). For the purposes of this

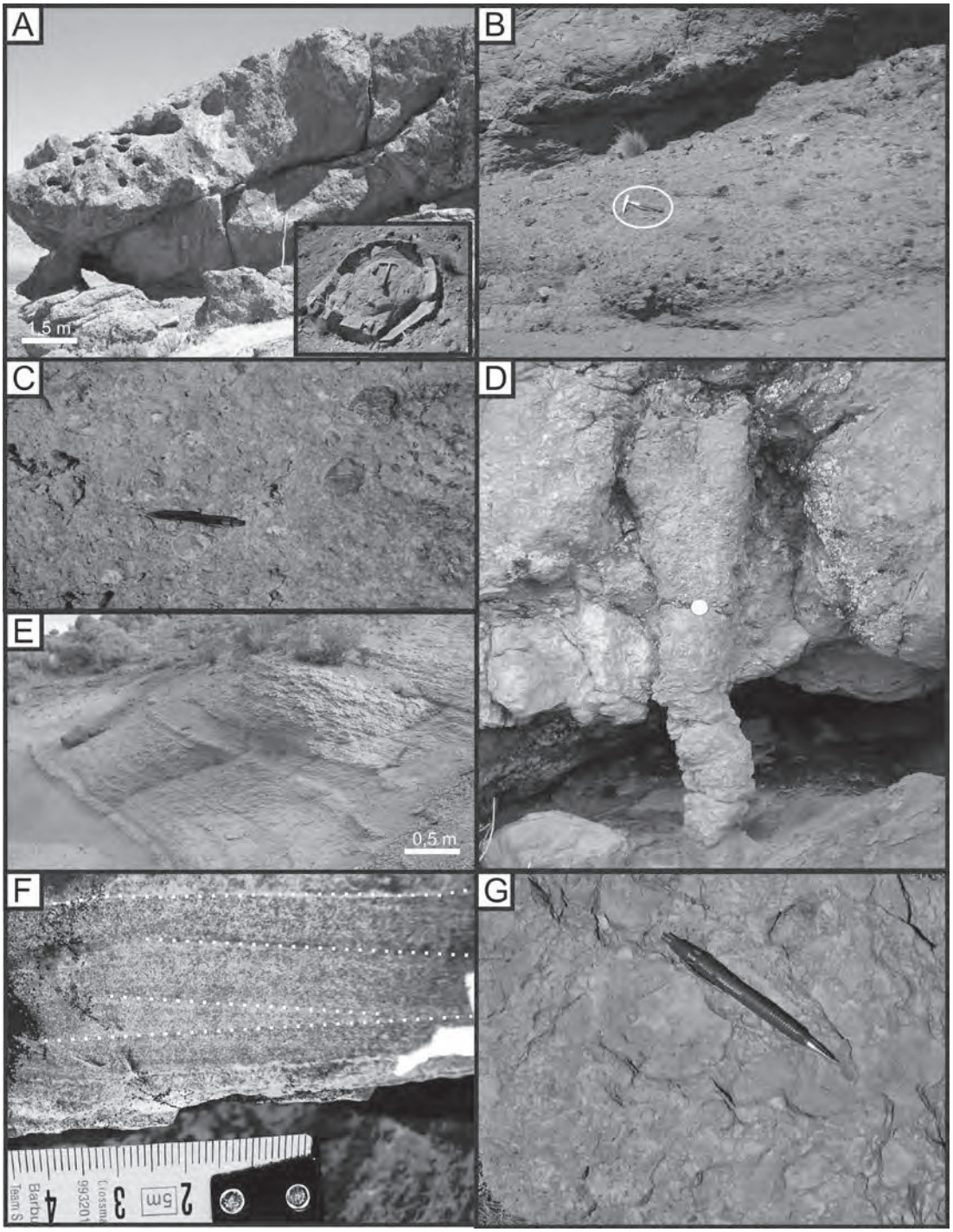

FIG. 5. Pyroclastic facies. **A.** Massive lithic breccias (*mBr*) in tabular bodies originated by block and ash flow (right corner, detail of juvenile andesitic clast). (B-F) Photographs of pyroclastic current deposits; **B.** Diffuse stratified lithic breccia lithofacies (*dslBr*; circle indicates a hammer for scale); **c .** Isotropic massive lapilli-tuff (*mLTi*) with scattered lithoclasts; **D.** Gas pipe in massive lapilli-tuff (*mLT*; coin for scale); **E.** Outcrop-scale photograph of diffuse-stratified lapilli-tuff (*dsLT*); **F.** Photographic detail of cross-bedded tuff facies (*xsT*)-dotted lines indicate the stratification-; **G.** Photographic detail of massive pumice lapillistone (*pmL*) originated by fall-out processes.

contribution, the use of the term 'volcaniclastic' is restricted to the original definition (Fisher, 1961 in Fisher and Schmincke, 1984): deposits composed predominantly of volcanic particles. To define the relationship between sedimentary environments and the volcanic setting, a provenance analysis was carried out, determining the monomictic or polymictic composition and clast-forming processes of the deposits (*i.e.*, monomictic ash-rich, monomictic lava-rich, polymictic volcaniclastic or polymictic epiclastic facies). According to these concepts, eleven siliciclastic lithofacies and two carbonate facies have been defined (Fig. 3). Siliciclastic lithofacies are the most common sedimentary facies within the syn-rift successions (Figs. 7A and 8A). Most of the siliciclastic facies within the studied succession show an absence of tractional structures. Therefore, this feature reveals the prevalence of transport and deposition from sediment gravity flow processes occurring in the syn-rift sequence (Fig. 3). The massive matrix-supported to clast-supported breccia facies *(Brmm)*, with large megablocks within an unsorted monomictic andesitic matrix with different degrees of fragmentation (Fig. 6A, C), has characteristic features of volcanic avalanche debris flow deposits (Schneider and Fisher, 1998; Clavero *et al*., 2002; Bret *et al*., 2003; Bernard *et al*., 2009). The massive matrix-supported conglomerate facies *(Gmm)* can be differentiated from avalanche deposits by their better sorting, their lobate or tabular pattern and the significantly smaller height and width of their outcrops (Fig. 6B). These characteristics suggest debris flow deposits (Coussot and Meunier, 1996; Bernard *et al*., 2009). The massive clast-supported breccia facies *(Brm;* Fig. 6G*)* and the massive to horizontally stratified clast-supported conglomerate facies *(Gm;* Fig. 6D*)*, which show a polymodal matrix and an absence of tractional structures, as well as the horizontally stratified pebbly sandstone/sandstone facies *(SGh/Sh(a);* Fig. 6F*)* and the massive sandstone facies *(Sm)*, which present massive or horizontal stratification with major transitional boundaries, suggest the accumulation of gravelly and sandy hyperconcentrated sheet flow deposits as a result of rapid deposition from sediment-laden currents (Smith, 1987; Smith and Lowe, 1991). The large-scale cross stratified clast-supported conglomerates facies *(Gp(b))* is composed at the same conglomerates facies that constituted the Gm lithofacies, developed in tabular bodies, with irregular bases which show large-scale foresets of 2 m to 3 m thick (Fig. 6E). The medium-scale cross-stratified clast-supported conglomerate facies *(Gp(a)),* and the cross-stratified sandstone facies *(Sx)* form lenticular bodies with erosive, concave bases. These bodies represent channel-fill deposits (Miall, 2006), associated with bedload transport and deposition from stream flows. The horizontally laminated sandstone facies *(Sh(b))* with tabular bodies suggest sheet flood deposits in upper-flow regime conditions (Miall, 2006). The horizontally laminated siltstone facies (*Fl;* Fig. 6H) may represent settling from suspensions in low-energy water bodies (Miall, 2006).

On the basis of the provenance analysis, the facies discussed above showed different compositional features. The *Brmm, Brm* and *Sm* facies present only a monomictic volcaniclastic composition (*Brmm*, monomictic andesitic composition; *Brm* and *Sm*, monomictic pyroclastic composition, *i.e*., pumiceous breccias and tuffaceous sandstones). The *Gmm, Gm, Gp(a), SGh/Sh(a)* and *Sx* facies present three different compositional types: monomictic andesitic composition, polymictic volcaniclastic composition or polymictic epiclastic composition (volcanic and basement lithoclasts), while the *Gp(b)* and *Sh* facies are constituted by polymictic epiclastic conglomerates.

The compositional features of the epiclastic facies reveal different degrees of relationship between the sediments fed to the sedimentary systems and the characteristics of the volcanic landscapes. The monomictic compositions generally suggest both a rapid resedimentation in syn-eruptive (effusive or explosive) stages (McPhie *et al*., 1993) and poorly integrated drainage networks, whereas a polymictic volcaniclastic composition represents a reworking and deposition during either minor syn-eruptive or inter-eruptive periods with poorly integrated drainage networks. The polymictic epiclastic compositions are constituted by an admixture of volcanic and igneous-metamorphic fragments originated by the erosion of basement rocks as well as the ones that constitute the syn-rift succession. This feature indicates integrated drainage networks and a decreasing volcanic supply to the depocentre.

The carbonate lithofacies (Fig. 3) are more restricted and localized than the other lithofacies, being developed towards the top of the syn-rift sequence (Fig. 7A). The carbonates are always extremely silicified and show a very low preservation of their primary sedimentary features, which generally occur

interbedded with the *Fl* lithofacies. The horizontally laminated limestone facies *(Ll(a);* Fig. 6I*)* and the microbial laminated limestone facies *(Ll(b))* may be interpreted as the non-marine precipitation of carbonates in shallow water bodies (Riding, 2000). The microbial laminated limestone facies *(Ll(b);* Fig. 6H, I*)* represents stromatolitic deposits in low-energy condition with little or no sediment supply (Talbot and Allen, 2002).

5. Spatial distribution of the lithofacies within the syn-rift sequence in the Sañicó depocentre

The stratigraphic and facies analyses reveal the large volume of effusive and explosive volcanic products within the Sañicó Formation, which constitute up to 72% of the syn-rift succession. Furthermore, different mechanisms of transport and deposition, as well as complex interplays between volcanic materials and sedimentary facies, were established (Fig. 3). Systematic vertical and lateral variations in the distribution of the volcanic and sedimentary lithofacies (Figs. 7A and 8A) indicate changes in the tectonic and volcanic controls during the syn-rift evolution. The tectonostratigraphic evolution can be recognized on the basis of the prevailing volcanic rocks in close relation with the four different compositional types of epiclastic facies documented throughout the syn-rift sequence. As a result, three informal sections can be devised: a lower section, middle section and upper section (Figs. 7A, B and 9). Volcanic rocks are volumetrically the most important in the lower and middle sections, while they are less frequent in the upper section of the syn-rift succession (Fig. 7A).

The lower section is mainly characterized by andesitic lava rocks and andesitic-dominated volcaniclastic rocks (monomictic andesitic composition and polymictic volcaniclastic composition). To a lesser extent, rhyolitic/rhyodacitic lavas and pyroclastic current deposits occur (Fig. 7A and 8A). This section was deposited in a highly compartmentalized depocentre, as depicted by large thickness variation and a high degree of preservation both beyond the boundaries of the depocentre and within it (Fig. 7A). Transverse to the faulted margins of the depocentre in the footwalls of the Cerro Michal and Cerro Corona fault systems, this section is composed of a thin succession of coherent and autobrecciated andesitic lava flows and lava domes (*cA+aA* facies) and dike swarms *(cA)* oriented parallel to the boundary fault systems. Towards the hanging walls, the section becomes thicker, reaching its maximum thickness close to the Cerro Michal fault system (1,100 m). In the hanging walls, the sections are constituted by large successions of coherent and autobrecciated andesitic lava flows (*cA+aA* facies) that prevail towards the base, and pyroclastic current deposits and gravity flow-dominated deposits towards the top (Fig. 7A). In some cases, andesitic lava domes and dikes (*cA±aA* facies), rhyodacitic lava domes (*cRD* facies) and dacitic necks (*cD* facies) associated with interior faults occur. The pyroclastic current deposits (*mLT+dsLT±mlBr±xT* facies) appear as huge lenticular bodies with their axes perpendicular to the boundary fault systems (Fig. 8A, B). The sedimentary lithofacies appear associated in different types of units. Volcanic debris avalanche deposits and debris flow deposits *(Brmm+Gmm)* are the dominating sedimentary lithofacies which occur as successions several decametres thick and hundreds of metres wide (Fig. 8A, B). To a lesser extent, major lenticular bodies several metres thick and hundreds of metres wide-mainly dominated by sandy and gravelly hyperconcentrated flow deposits *(Gm+SGh/Sh(a))*-were recorded (Fig. 8A). Inside them, tractional facies such as *Gp(a)* and *Sx* and debris flow deposits *(Gmm)* may occasionally appear. It is important to highlight that parallel to the boundary fault systems this section shows a change in thickness, reaching their minimum towards the tip point of the fault, in which the different facies onlap the basement rocks (Fig. 8A, B).

The middle section are mostly composed of thick rhyolitic/rhyodacite pyroclastic current deposits which appear intebedded with pyroclastic-monomictic volcaniclastic deposits and andesitic-rhyolitic lava flows and lava domes related to extensional faults (Figs. 7A and 9). The architecture of this section is very different from the lower section, prevailing only inside the depocentre (Fig. 9) and a more regular geometry and lateral continuity of the lithofacies are common. Pyroclastic current deposits crop out as laterally continuous units up to 350 m thick, constituting more than 85% of the volume of the middle section (Fig. 7A). At least three units of pyroclastic current deposits were recognized and they appear intercalated with either thin successions (<30 m thick) of pumice/tuff-rich hyperconcentrated flow deposits *(Brm+Sm)* or andesitic lava flows/lava domes *(cA+aA)* related to fractures (Fig. 7A). Pyroclastic

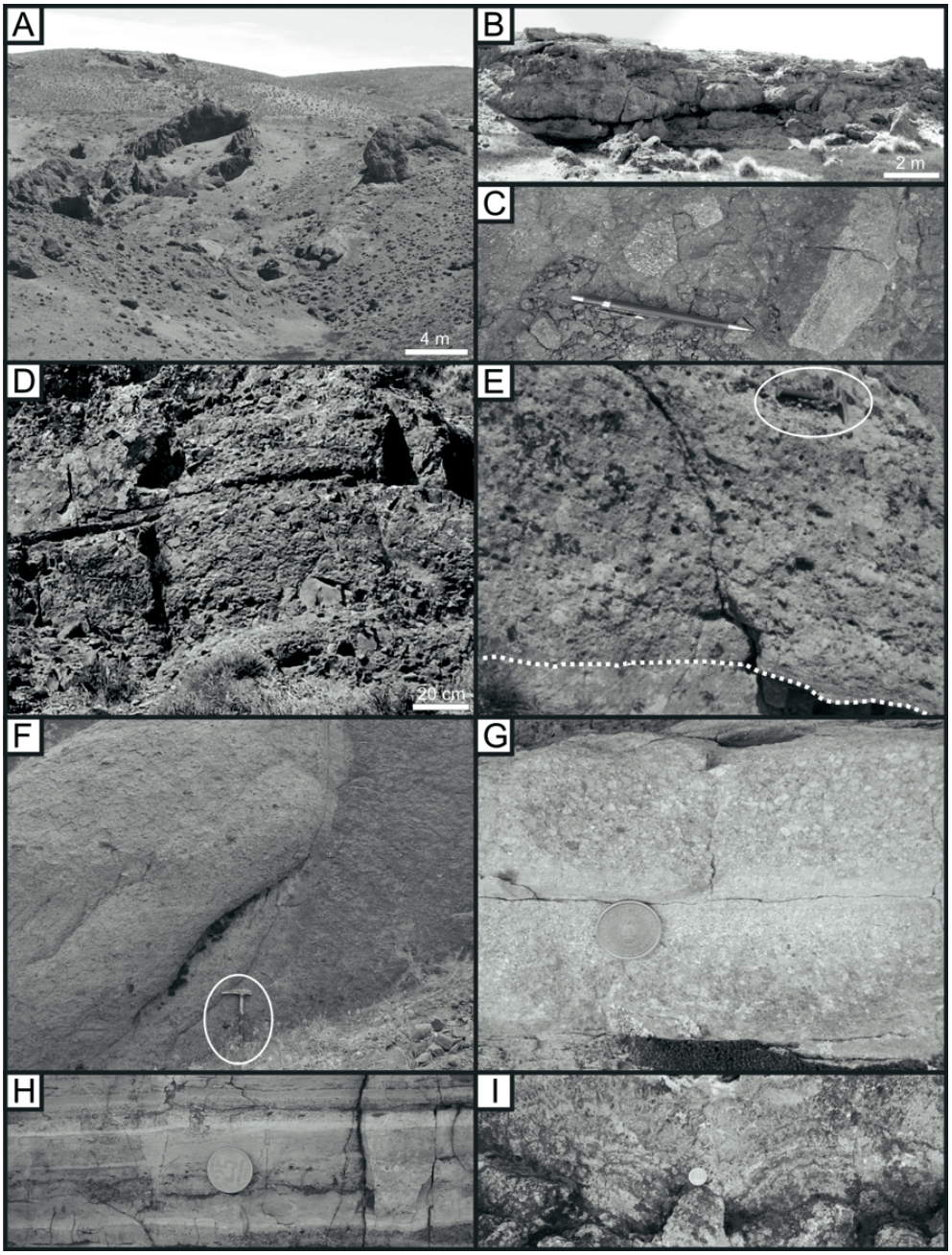

FIG. 6. Sedimentary lithofacies. (A-G) Siliciclastic facies. **A.** Outcrop scale-photograph of massive matrix-supported to clast-supported breccias (*Brmm*) formed by volcanic debris avalanche flows; **B.** Lobate body successions composed of massive matrix-supported conglomerates (*Gmm*) deposited from debris flows; **c .** Protographic detail of monomictic andesitic rocks with different textural arrangements; **D.** Tabular bodies formed by massive to horizontally stratified clast-supported conglomerates (*Gm*) originated by gravelly hyperconcentrated sheet flows; **E.** Tabular body with slightly erosive bases formed by large-scale cross-stratified clast-supported conglomerates *(Gp(b))*; **F.** Outcrop scale-photograph of sandy hyperconcentrated sheet flow deposits (*SGh*/*Sh(a)*; circle indicates a hammer for scale; **G.** Thin tabular bodies formed by massive clast-supported breccias (*Brm*) interpreted as pumiceous hyperconcentrated flow deposits. (H-I) Carbonate lithofacies. **H.** Photographic detail of horizontally laminated limestone facies *(Ll(a))* interbbeded with thin layers of horizontally laminated siltstones (*Fl*); **I.** Build-up structure developed in microbial laminated limestones *(Ll(b))*.

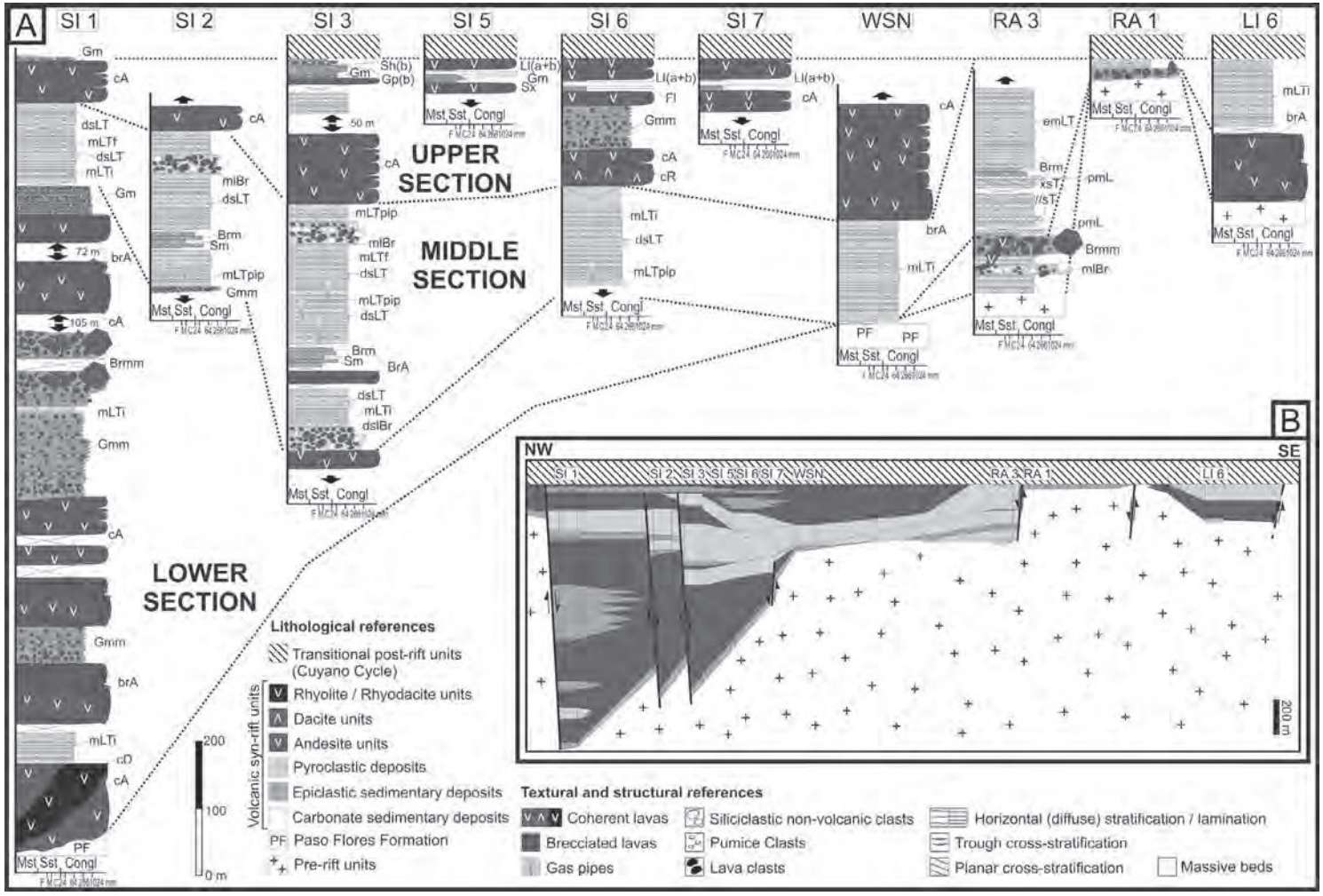

FIG. 7. Section logged for the rift succession of the Sañicó depocentre: **A.** Sedimentological logs transversal to the depocentre (see figure 3 for facies code). Not to scale horizontally, see figure 2 for location. Dotted lines indicate the correlation between the sections established. **Mst**: mudstones; **Sst**: sandstones; **c ongl**: conglomerates; **F**: fine; **M**: medium; **c** : coarse; **B.** Longitudinal correlation panel established from the logged sections SI 1–LI 6, showing the overall half-graben geometry and the distribution of the lithofacies of the depocentre (see lithological references in figure 7A). Location of the extensional faults is based on the geological map in figure 2.

units are lapilli-tuff-dominated (*i.e.*, *mLT+dsLT±// sT±xsT* facies) and in some cases show *pmL* facies at the base and *mlBr* facies at the base or in the middle part (Fig. 7A). Each of the pyroclastic units show large change in thickness related to both internal and boundary faults of the depocentre (Fig. 7A, B) during the eruptive events. These structural features not only controlled the accommodation for these units, but also the distribution of internal lithofacies, causing the deposition of *mlBr* facies close to the boundary fault systems of the depocentre (Fig. 7A). Towards the top of this section, scarce rhyolitic lava flows (*cR±aR*) related to fractures were recorded (Fig. 7A).

The upper section of the syn-rift sequence is characterized by a decrease in the volume of the volcanic rocks (<55%), as well as a reduction of the accommodation space, presenting a more limited distribution and less thickness in the depocentre (Figs. 7A, B and 9). It is composed of andesitic lava flows with epiclastic (*i.e.*, polymictic volcaniclastic and polymictic epiclastic facies) and carbonate sedimentary rocks. These lithofacies are asymmetrically distributed both laterally and vertically within the depocentre (Fig. 7A, B). Close to the hanging wall of the Cerro Corona boundary this section is constituted by coherent, and to a lesser extent autobrecciated, andesitic lava flow (*cA±aA*) successions up to 250 m thick. On the other side of the depocentre, near the Cerro Michal fault system hanging wall, this section is constituted by coherent andesitic lava flows (*cA*) intercalated with epiclastic and carbonate deposits (Fig. 7A). Towards the base, the epiclastic facies composed of debris flow deposits with a polymictic volcaniclastic provenance have a large distribution. Towards the top, polymictic epiclastic and carbonate facies interbebbed with thin coherent andesitic lava flows (*cA*) occur. Close to the Cerro Michal boundary, polymictic epiclastic rocks are developed as tabular bodies composed of large-scale cross-stratified conglomerates *(Gp(b))* with *Gm* and *Sh(b)* lithofacies (Fig. 7A). These bodies form sequences up to 5 m thick with coarsening-upward grain-size trends that can be related to gradual changes in the depositional processes. Towards the inner depocentre,

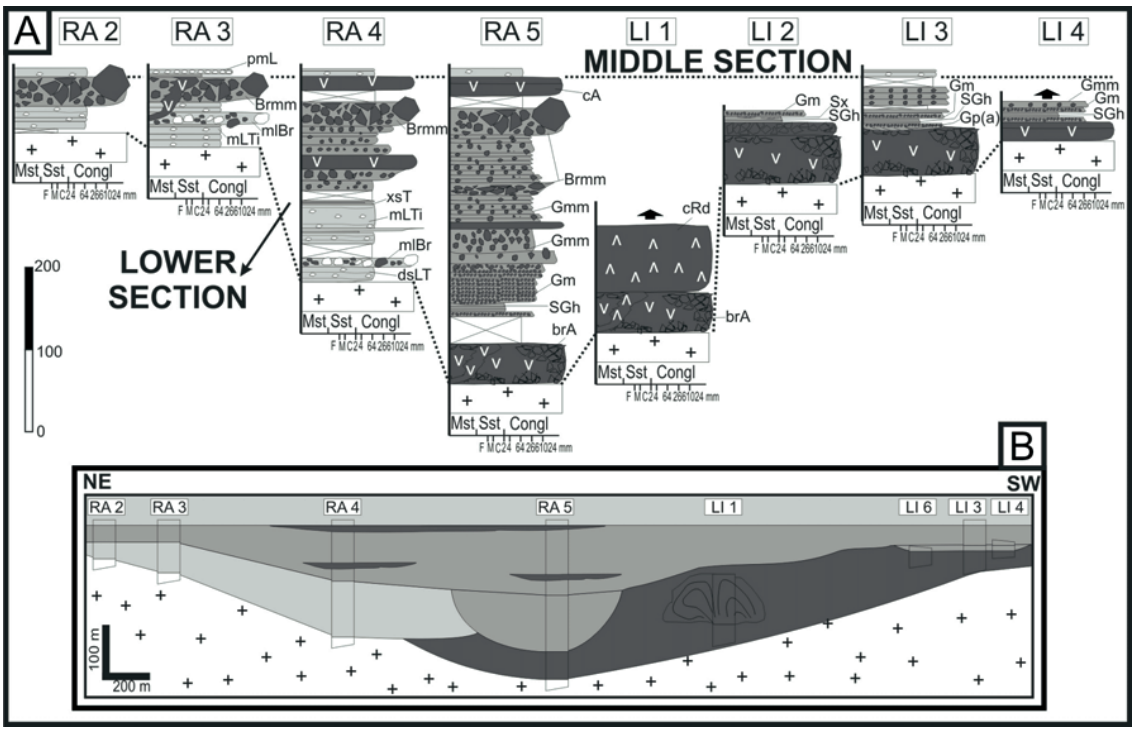

FIG. 8. Sedimentological logs for the volcanic syn-rift of the Sañicó depocentre. **A.** Sedimentological logs parallel to the Cerro Corona fault system; **B.** Longitudinal correlation panel of the logged sections RA 2-LI 4, showing the lithofacies distribution. Dotted lines in A indicate the correlation between the sections established (for references, see figure 7).

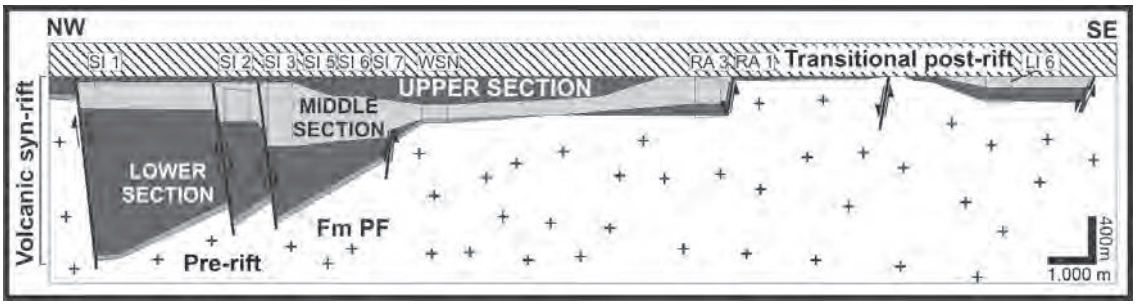

FIG. 9. Lateral and vertical distribution of sections defined for the syn-rift sequence in the Sañicó depocentre (see figs. 3 and 7 for the location and details of the logged sections).

these facies turn into a thin succession of limestones *((Ll(a)+Ll(b))* and fine-grained siliciclastic deposits (*Ll*) with minor *Sx* lithofacies.

6. Discussion: evolution and tectonostratigraphic controls over the volcanic syn-rift sequence

The fault systems of the Sañicó depocentre controlled the accumulation of a thick syn-rift succession, in the hanging wall of the main boundary fault of the depocentre (Cerro Michal fault system; Figs. 7A, B and 9). Although the stratigraphic analysis constrained the syn-rift to the Hettangian-Sinemurian (*i.e.*, Sañicó Formation; Stipanicic, 1967; Stipanicic *et al*., 1968), a recent geochronological study developed close to the studied area, constrained this volcanic syn-rift sequence to the Sinemurian age (*i.e.*, 191,7±2,8 Ma to Pliensbachian age; Spalletti *et al*., 2010), representing a total period of approximately 4 Ma.

Stratigraphic and facies analysis determined the main component of the syn-rift sequence with their hydrodynamic and rheological mechanisms of transport and deposition (Fig. 3). In order to establish the tectonostratigraphic framework of the Sañicó depocentre, three sections were defined on the basis of the prevailing volcanic rocks in close relation with the four different compositional types of epiclastic facies documented (Figs. 7A and 9). Thus, the relationships and architectural patterns between the lava, pyroclastic and sedimentary components that constitute the syn-rift sequence were determined (Figs. 7B and 8B). The change in the amount of volcanic versus sedimentary materials, the variations in the composition and mechanisms of transport and deposition of the sedimentary facies, and different tectonic and volcanic controls over the fill are the key elements that marked the signature of each section. Therefore, the tectonostratigraphic evolution of the syn-rift succession in the Sañicó depocentre may be carried out by means of the analysis of each section. These sections in turn represent three major evolutionary stages of the volcanic syn-rift sequence: the early-rift stage, mid-rift stage and late-rift stage.

The early-rift stage (lower section) corresponds to the onset of the syn-tectonic infill of the Sañicó depocentre, which is characterized by a volcano-sedimentary wedge dominated by effusive volcanic products and volcaniclastic rocks (Figs. 7A, 8A and 9) caused by the resedimentation and reworking of the former. During this stage the syn-rift units are wedge-shaped and highly compartmentalized with large thickness variations indicating a half-graben geometry (Fig. 7). This condition is common in the early evolution of the rift basin (Gawthorpe and Leeder, 2000; Morley, 1999a). Volcanic rocks compose up to 61% of the section, showing a discernible polarity with the sedimentary deposits (Fig. 7A). In the footwalls of the boundary fault systems of the depocentre, this section is composed of a thin succession of lava flows, lava domes and dike swarms (*cA+aA* facies), whereas towards the hanging walls it is formed by a large succession of lava flows (*cA+aA* facies), pyroclastic current deposits and gravity flow-dominated deposits (Fig. 7A). To a lesser extent, dikes, lava domes and necks of diverse composition are present. The huge lenticular bodies of pyroclastic current deposits (*mLT+dsLT±mlBr±xT* facies) represent the filling of paleovalleys (Fig. 8A) from short-lived granular fluid-based pyroclastic density currents caused by simple-pulse collapse from pyroclastic column (Branney and Kokelaar,

2002). The sedimentary lithofacies with andesitic dominated provenance, that is, the volcanic debris avalanche deposits and debris flow deposits (*i.e.*, *Brmm+Gmm*) and the major lenticular bodies dominated by hyperconcentrated flow deposits (*i.e.*, *Gm+SGh/Sh(a)±Gp(a)±Sx±Gmm*), suggest short- and long-lived degradational stages of the volcanic landscapes (Davidson and De Silva, 2000) due to alluvial processes (*sensu* Blair and McPherson, 1994) in either syn-eruption or inter-eruption periods with less integrated drainage networks (Palmer *et al*., 1993; Zanchetta *et al*., 2004). Most of the features of the volcanic and sedimentary units defined herein were described for many composite volcanoes in the world, such as the compositional range from andesitic to rhyodacitic products dominated by thick andesitic lava successions (Cas and Wright, 1987), the pyroclastic current deposits that filled valleys (Davidson and De Silva, 2000), major degradational events composed of volcanic debris avalanches (Schneider and Fisher, 1998; Reubi and Hernández, 2000; Belousov *et al*., 1999; Clavero *et al*., 2002; Shea *et al*., 2008), large channelized volcaniclastic alluvial units (Palmer *et al*., 1993; Zanchetta *et al*., 2004) and minor acid lava domes and necks (*cRD*, *cD* facies) that worked as satellite vents (Davidson and De Silva, 2000). The characteristics of this units and their polarity within the depocentre suggest that during the early-rift stage composite volcanoes occurred on the boundary of the Sañicó half-graben (Fig. 10).

The evolution of the syn-rift sequence was followed by the mid-rift stage (middle section), which is pyroclastic-dominated (Fig. 7A). The syn-rift deposits of this stage are recorded only inside the depocentre and, although it presents thickness changes related to internal faults, more regular geometries are common (Figs. 3, 7 and 9). The middle section is mainly composed of thick acid pyroclastic current deposits intebedded with thin pumiceous and ash-rich volcaniclastic deposits and andesitic-rhyolitic lava units related with extensional faults. The internal and boundary faults of the depocentre (Figs. 3 and 7) controlled the thickness changes and facies distribution of the pyroclastic units during the eruptive events. This reveals that previous faults worked as volcano-tectonic extensional faults during the eruptive events. At least three volcano-tectonic periods were recorded on the basis of the occurrence of large-pyroclastic current deposits that choked the accommodation space of the depocentre. The distribution and internal facies arrangement of the lapilli-tuff-dominated pyroclastic current deposits (*i.e.*, *mLT+dsLT±//sT±xsT±pmL±mlBr* facies) suggest that they originated as a result of long-lived, sustained, quasi-steady, granular fluid-based pyroclastic density currents, due to complex-pulse collapse from pyroclastic column Branney and Kokelaar, 2002). The ignimbrite deposits are interbedded with andesitic lava flows/lava domes *(cA+aA)* mainly related to fractures and thin successions of pumiceous and ash-rich hyperconcentrated flow deposits (*Brm+Sm*). This assemblage may indicative of rapid resedimentation from alluvial processes, common in syn-eruptive stages and poorly integrated drainage networks (Smith, 1986; Smith, 1991; Smith and Lowe, 1991; Muravchik *et al*., 2011). Both units indicate that the volcano-tectonic events were not only related with asymmetric subsidence, but also with episodic subsidence. Some authors classify this kind volcanic edifice as volcano-tectonic depressions (Moore and Kokelaar, 1997; Moore and Kokelaar, 1998; Lipman, 2000). These types of calderas were recorded in different extensional or transtensional settings related to magmatism in the world (the Scafell caldera, Branney and Kokelaar, 1994; the Glencoe Graben, Moore and Kokelaar, 1997; Moore and Kokelaar, 1998; the Long Valley caldera, Cole *et al*., 2005; the Taupo and Okataina calderas, Spinks *et al.*, 2005; the Sierra Madre Occidental caldera, Aguirre-Díaz *et al*., 2008; the Cerro Aguas Calientes caldera; Petrinovic *et al.*, 2010). Therefore, a volcano-tectonic depression related with asymmetrical and incremental subsidence was superimposed during the mid-rift stage of the Sañicó depocentre (Fig. 10).

The late-rift stage (upper section) records a decrease in the volume of volcanic rocks and a reduction of the accommodation space (Figs. 7, 9 and 10). During this period, andesitic lava units with epiclastic and carbonate sedimentary rocks were asymmetrically distributed both laterally and vertically within the depocentre. Close to the hanging wall of the Cerro Corona boundary (Fig. 7), low-relief effusive aggradational volcanic edifices and lava fields may be interpreted on the basis of a coherent, and to a lesser extent autobrecciated, andesitic lava flow (*cA±aA*) succession (Brown and Bell, 2007). On the other side of the depocentre (Fig. 7), at the base of this section, near the Cerro Michal fault system hanging wall, coherent andesitic lava flows *(cA)* interbedded with epiclastic polymictic volcaniclastic debris flow

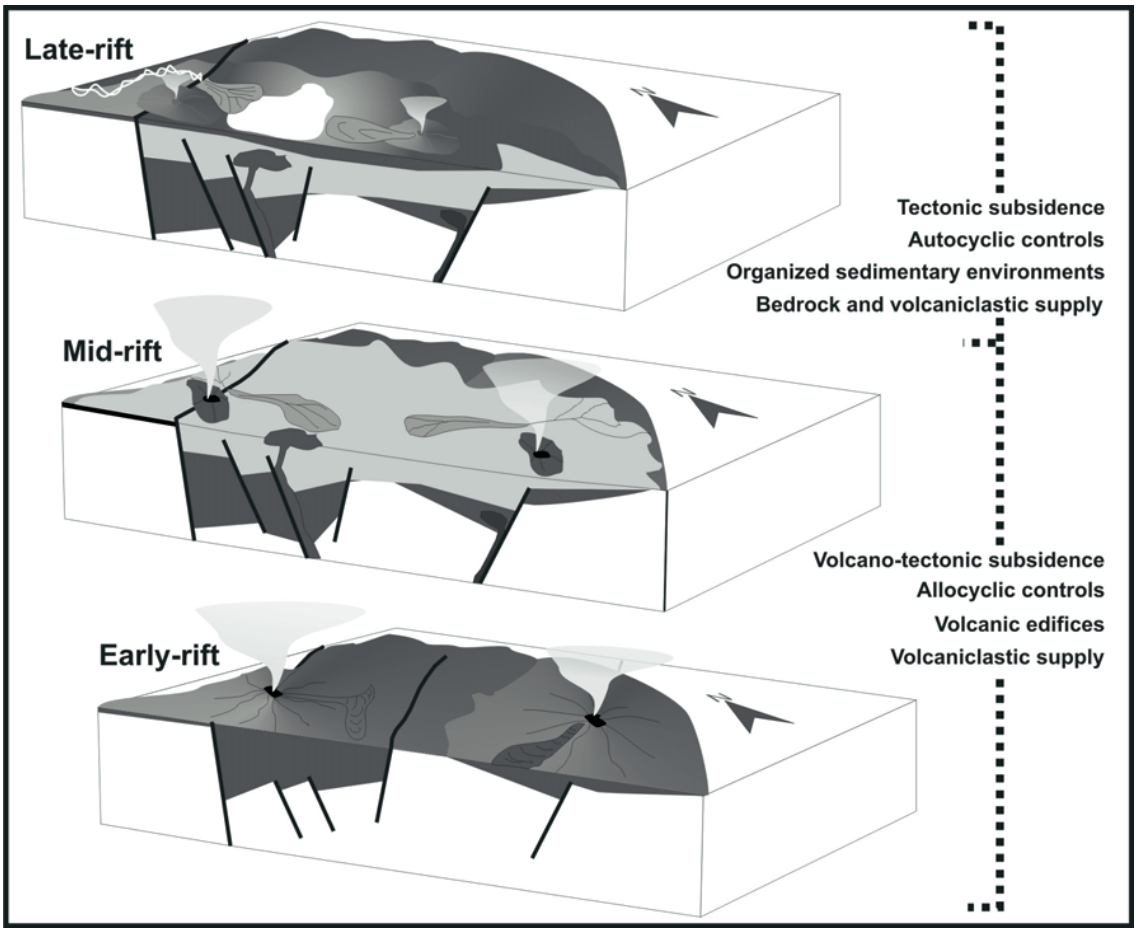

FIG. 10. Conceptual models showing the tecto-stratigraphic evolution of the Sañicó depocentre with the main controls over the syn-rift sequence. To the right, the dotted line indicates the predominant parameters identified in the different stages of the volcanic syn-rift.

deposits indicate low-relief effusive aggradational volcanic edifices and lava fields (Brown and Bell, 2007) with highly integrated drainage networks as a result of the erosion and reworking of the different volcanic rocks of the syn-rift. Towards the top of the section (Fig. 7), thin coherent andesitic lava flows with epiclastic and carbonate facies are developed. Tabular bodies characterized by large-scale cross-stratified conglomerates (*Gp(b)+Gm+Sh(b)* facies) suggest a coarse-grained delta front and alluvial facies (Reading and Collinson, 2002; Blair and McPherson, 2008). The polymictic epiclastic compositon of these facies indicates highly integrated drainage networks and less influence of active volcanism. Towards the inner depocentre, the sedimentary environment turns into a thin succession of limestones and fine-grained siliciclastic deposits interpreted as shallow lacustrine units (*i.e*., *Ll(a)+Ll(b)+Ll;* Talbot and Allen, 2002) with underflow deposits *(Sx)* in a prodelta to off-shore lacustrine position (Reading and Collinson, 2002; Blair and McPherson, 2008; Rohais *et al*., 2008).

Most of the studies of rift-basins were made for non-volcanic extensional depocentres (*e.g*., Schlische, 1991; Schlische, 1992; Morley, 1995; Schlische and Anders, 1996; Gawthorpe and Leeder, 2000; Gawthorpe *et al*., 2003; Young *et al*., 2003; Morley *et al*., 2004; Jackson *et al*., 2005), which is why they do not discuss the interrelationships between the tectonic structures and volcanism, the large volume of volcanic and volcaniclastic materials provided to the depocentres, the aggradation above the geomorphologic threshold, and the lateral and

vertical variations of environments in these places. The tectonostratigraphic framework given above showed how these tectonic and volcanic variables were present in different magnitudes and times during the syn-rift evolution.

The tectonic controls over the syn-rift sequence are shown at different scales. The Sañicó depocentre may be classified as a volcanic half-graben with a NW-SE orientation and oblique internal tectonic features (Figs. 3 and 7). According to the pervasive and isolated fabrics suggested by some authors (Varela *et al*., 1991), the external and internal structural configuration of the depocentre seems to be inherited from pre-existing fabrics of the basement. This condition has been recognized for the Neuquén Basin (Franzese and Spalletti, 2001) and other Gondwanic basins (*e.g*., Cuyo Basin; Ramos and Kay, 1991), as well as for other extensional basins in the world (Morley, 1999b; Moustafa, 2002; Morley *et al*., 2004). Although recent studies have shown an almost unidirectional large-scale pattern (NNW-SSE) for the initial depocentres (Cristallini *et al*., 2006; Giambiagi *et al*., 2008a; Giambiagi *et al*., 2008b; Giambiagi *et al*., 2008c, Cristallini *et al*., 2009), related to NNE regional extension (Bechis *et al*., 2010), a similar orientation to those of the Sañicó depocentre were indicated for the early stage of the Neuquén Basin (*e.g*., Sierra de Chacaico; Franzese *et al*., 2007; Sierra de Reyes and Sierra de Cara Cura; Giambiagi *et al*., 2008a; Giambiagi *et al*., 2008b). On a smaller scale, the extensional faults not only controlled the accommodation space of the depocentre, but also provided magma pathways to the surface and a focus for dike emplacement (*e.g*., volcanic necks and dike swarms), which could have contributed to the rift extension (Abebe *et al*., 2007; Spinks *et al*., 2005; Cassidy *et al*., 2009). Thus, the tectonic control was a major feature at the location of the volcanic building (*i.e*., composite volcanoes on the boundary of the depocentre), taking over at the same time the polarity of the sedimentary facies in both the volcano-dominated stages of the syn-rift (*e.g*., lower section) and a sedimentary-dominated stage of the syn-rift (*i.e*., upper section).

The main volcanic controls documented in the syn-rift sequence may be summarized as the superimposition of magmatism with tectonic features and the influence of such controls over the volcanic landscapes and sedimentary environments. The superimposition of magmatism with tectonic features is indicated by the repeated volcano-tectonic episodes recorded. They suggest the recurrent plumbing of magmas along the Sañicó depocentre and the magma-chamber roof collapse causing the formation of a polygonal caldera (*i.e*., mid-rift stage; Fig. 10), usually identified in extensional settings of this kind (Spinks *et al*., 2005). In order to establish the influence of the volcanic controls on the effect of the ancient landscapes, the interrelations between the magmatic systems with the upper part of the crust is an essential aspect to be considered (Cas and Wright, 1987; Németh and Ulrike, 2007). As examples, constructional volcanic edifices interpreted during the early-rift stage (*i.e*., composite volcanoes) controlled the distribution of the volcanic materials beyond the limit of the depocentre (Fig. 10), whereas an excavational volcanic building identified for the mid-rift stage (*i.e*., volcano-tectonic depressions) controlled the preservation of pyroclastic deposits within the depocentre (Fig. 10). Finally, the degree of volcanic activity and the types of eruption processes (*i.e*., effusive or explosive) are also important elements to be considered in order to determine their effects over the sedimentary paleoenvironments of the syn-rift sequence. During high volcanic supply, the overfilled condition of the depocentre caused disordered stacking of the sedimentary successions (*e.g*., lower and middle sections). Besides, the effusive- or explosive-dominated eruptive processes within the syn-rift sequence controlled the grain size of the volcaniclastic debris provided to the depocentre (*e.g*., coarse-grained during effusive periods, and tuffaceous fine-grained during the explosive stages). On the other hand, the decrease in volcanic supply identified in the upper section caused the development of well-organized stacking patterns in the sedimentary sequences (*e.g*., coarsening-upward succession of delta front deposits), a better arrangement of the sedimentary environment, and highly integrated drainage networks.

An integrated model may be suggested for the Sañicó depocentre which developed around 4 Ma during Sinemurian age. The onset of the rift sequence began with the development of a highly compartmentalized half-graben depocentre simultaneously with a growth of polygenetic constructional volcanic edifices in boundary position (*i.e*., composite volcanoes defined in the lower section; Fig. 10). Subsequently, volcano-tectonic subsidence events were superimposed, originating polygonal

calderas (Fig. 10). Finally, minor volcanic edifices with an organized sedimentary environment were developed during the end of the volcanism and the extensional event (Fig. 10). It is important to highlight that on the basis of similar stratigraphic patterns recorded in other depocentres of the basin (Pángaro *et al*., 2002; Franzese *et al*., 2006; Franzese *et al*., 2007; Llambías *et al*., 2007; D'Elia *et al*., 2012), as well as in other volcanic extensional basins in the world (*e.g*., the volcanic Taupo zone; Price *et al*., 2005; Rowland *et al*., 2010), it can be stated that this model could be useful to characterize the volcanic-rift depocentres at the onset of the Neuquén Basin.

Other remarkable issue is the evolution of the depocentre in relation to the large-scale Upper Triassic-Lower Jurassic extensional event and how classical stratigraphical units of this age are grouped within the rifting event. In this case it is possible that the Upper Triassic Paso Flores Formation is related to the first-order extensional event that originated de Neuquén basin, but certainly is not related with the tectonostratigraphic evolution of the Sañicó depocentre. This indicate that, at least, there are two future topics that must pay attention: **a**. accurate evolution time of the isolated depocentres of the basin-in this case approximately 4 Ma- and **b**. the possibility of total reorganization of the accommodation space between different syn-rift event during the rifting.

7. c onclusions

The Sañicó depocentre is a extensional half-graben with a NW-SE orientation and oblique internal tectonic features that were active during the early rifting of the Neuquén Basin. The graben border system of the Sañicó half-graben was controlled by the Cerro Michal fault system and its associated structures. The syn-rift fill in the Sañicó area constitutes a complex arrangement of units very diverse in nature in which volcanic rocks compose up to 72% of the infill. The stratigraphic and facies analysis established the different components of the syn-rift sequence, *i.e*., lava, pyroclastic and sedimentary deposits. The predominance of these was identified in different parts of the fill. The main mechanisms of transport and deposition identified are lava flows, pyroclastic currents and sediment gravity flows. The tectonostratigraphic analysis revealed that the evolution of the syn-rift sequence in the Sañicó depocentre may be considered in three sections (the lower, middle, and upper sections) characterized by the predominance of effusive, pyroclastic or sedimentary rocks and distinct architectural patterns. The signature of each stage of the syn-rift evolution mainly depends on the change in the amount of volcanic versus sedimentary products in close relationship with the structural features of the depocentre. The onset of the syn-tectonic infill of the Sañicó depocentre (lower section) was characterized by andesitic-rhyodacitic lava flows with the predominance of thick andesitic lava sequences, pyroclastic current deposits that filled valleys, major degradational events composed of volcanic debris avalanches, large channelized volcaniclastic alluvial units and minor acid lava units that worked as satellite vents. The arrangement and distribution of these units may be interpreted as composite volcanoes on the boundary of the Sañicó depocentre. The evolution of the syn-rift sequence continued with the development of fault-controlled, large ignimbrite deposits with an acid composition, intebedded with volcaniclastic alluvial deposits and andesitic-rhyolitic lava units related to extensional faults (middle section), which suggests a volcanotectonic depression related with asymmetrical and incremental subsidence. The end of this syn-rift event was marked by a decrease in the volume of volcanic rocks, a reduction of the accommodation space and the development of highly integrated drainage networks. During this period (upper section), low-relief effusive aggradational volcanic edifices and lava fields in close relation with alluvial, deltaic and lacustrine units occurred.

The analysis of the syn-rift sequence in the Sañicó depocentre determined the complex relationships between tectonic and volcanic variables, occurring in different magnitudes and times during the syn-rift evolution. The tectonic and volcanic controls over the syn-rift sequence were established at different scales, affecting the accommodation space, the magma-feeding systems, the types and location of the volcanic buildings, as well as the polarity, types and distribution of syn-rift deposits.

On the basis of facies and tectonostratigraphic analyses, a conceptual model was devised to understand the relationships between volcanism and extensional tectonics, which could be useful to characterize the volcanic-rift depocentres of the Neuquén Basin.

Acknowledgements

The authors would like to thank the people of the Sañicó area for their support and hospitality. We are especially grateful to F.E. Zamora and C.M. Freire of the Estancia La Inmaculada, to M. Carullo of the Estancia Santa Isabel and to the Torres family of the Ancatruz community for allowing us access to the outcrops and for their kind generosity. The authors would also like to especially thank G. Veiga, A. Bilmes, I. Cambon, D. Disalvo and M. Hernández for their assistance in the field and their friendship. We also want to thank the reviewers, V. Ramos and A. Folguera, for their comments that improve the quality of a work. This research was funded by the Agencia Nacional de Promoción Científica y Tecnológica (PICT 07-8451; PICT 2530-BID 1728/OC-AR).

References

Abebe, B.; Acocella, V.; Korme, T.; Ayalew, D. 2007. Quaternary faulting and volcanism in the Main Ethiopian Rift. Journal of African Earth Sciences 48: 115-124.

Aguirre-Díaz, G.J.; Labarthe-Hernández, G.; Tristán-González, M.; Nieto-Obregón, J.; Gutiérrez-Palomares, I. 2008. The ignimbrite flare-up and graben caldera of the Sierra Madre Occidental, Mexico. *In* Caldera Volcanism: analysis, modeling and response (Gottsmann, J.; Martí, J.; editors). Elsevier: 143-174.

Álvarez, P.P.; Ramos, V.A. 1999. The Mercedario rift system in the principal Cordillera of Argentina and Chile (32°LS). Journal of South American Earth Sciences 12: 17-31.

Bechis, F.; Giambiagi, L.; García, V.; Lanés, L.; Cristallini, E.; Tunik, M. 2010. Kinematic analysis of a transtensional fault system: The Atuel depocenter of the Neuquén basin, southern Central Andes, Argentina. Journal of Structural Geology 32: 886-899.

Belousov, A.; Belousova, M.; Voight, B. 1999. Multiple edifice failures, debris avalanches and associated eruptions in the Holocene history of Shiveluch volcano, Kamchatka, Russia. Bulletin of Volcanology 61: 324-342.

Bernard, B.; van Wyck de Vries, B.; Leyrit, H. 2009. Distinguishing volcanic debris avalanche deposits from their reworked products: the Perrier sequence (French Massif Central). Bulletin of Volcanology 71 (9): 1041-1056.

Best, M.G.; Christiansen, E.H. 2001. Igneous Petrology. Blackwell Science, Inc.: 460 p.

Bilmes, A.; Muravchik, M.; D'Elia, L.; Franzese, J.R. 2008. Interacción entre las secuencias sineruptivas e intereruptivas en los depósitos precuyanos del sinrift de la Cuenca Neuquina, Sierra de Chacaico, Neuquén. *In* Congreso Geológico Argentino, No. 17, Actas 2: 746-747. San Salvador de Jujuy.

Blair, T.C.; McPherson, J.G. 1994. Alluvial fans and their natural distinction from rivers based on morphology, hydraulic processes, sedimentary processes, and facies assemblages. Journal of Sedimentary Research 64: 450-489.

Blair, T.C.; McPherson, J.G. 2008. Quaternary sedimentology of the Rose Creek fan delta, Walker Lake, Nevada, USA, and implications to fan-delta facies models. Sedimentology 55: 579-615.

Branney, M.J.; Kokelaar, B.P. 1994. Volcanotectonic faulting, soft-state deformation, and rheomorphism of tuffs during development of a piecemeal caldera, English Lake District. Geological Society of America Bulletin 106: 507-530.

Branney, M.J.; Kokelaar, B.P. 2002. Pyroclastic density currents and the sedimentation of ignimbrites. Geological Society, Memoir 27: 144 p. London.

Bret, L.; Fevre, Y.; Join, J.; Robineau, B.; Bachelery, P. 2003. Deposits related to degradation processes on Piton des Neiges Volcano (Reunion Island): overview and geological hazard. Journal of Volcanology and Geothermal Research 123: 25-41.

Brown, D.J.; Bell, B.R. 2007. Debris flow deposits within the Palaeogene lava fields of NW Scotland: evidence for mass wasting of the volcanic landscape during emplacement of the Ardnamurchan Central Complex. Bulletin of Volcanology 69: 847-868.

Brown, R.J.; Kokelaar, B.P.; Branney, M.J. 2007. Widespread transport of pyroclastic density currents from a large silicic tuff ring: the Glaramara tuff, Scafell caldera, English Lake District, UK. Sedimentology 54 (5): 1163-1190.

Cas, R.A.F.; Wright, J.W. 1987. Volcanic successions: Modern and ancient. Chapman and Hall: 528 p. Londres.

Cassidy, J.; Ingham, M.; Locke, C.A.; Bibby, H. 2009. Subsurface structure across the axis of the Tongariro Volcanic Centre, New Zealand. Journal of Volcanology and Geothermal Research 179: 233-240.

Clavero, J.E.; Sparks, R.S.J.; Huppert, H.E.; Dade, W.B. 2002. Geological constraints on the emplacement mechanism of the Parinacota debris avalanche, northern Chile. Bulletin of Volcanology 64: 40-54.

Cole, R.B.; Milner, D.M.; Spinks, K.D. 2005. Calderas and caldera structures: a review. Earth Science Reviews 69: 1-26.

Coussot, P.; Meunier, M. 1996. Recognition, classification and mechanical description of debris flows. Earth-Science Reviews 40: 209-227.

Cristallini, E.; Bottesi, G.; Gavarrino, A.; Rodríguez, L.; Tomezzoli, R.; Comeron, R. 2006. Synrift geometry of the Neuquén Basin in northeastern Neuquén Province, Argentina. *In* Evolution of an Andean margin: a tectonic and magmatic view from the Andes to the Neuquén Basin (35°-39°S lat) (Kay, S.M.; Ramos, V.A.; editors). Geological Society of America, Special Paper 407: 147-161.

Cristallini, E.; Tomezzoli, R.; Pando, G.; Gazzera, C.; Martínez, J.M.; Quiroga, J.; Buhler, M.; Bechis, F.; Barredo, S.; Zambrano, O. 2009. Controles precuyanos en la estructura de la Cuenca Neuquina. Revista de la Asociación Geológica Argentina 65 (2): 248-264.

Damborenea, S.E.; Manceñido, M.O.; Riccardi, A.C. 1975. Biofacies y estratigrafía del Liásico de Piedra Pintada, Neuquén, R. Argentina. *In* Congreso Argentino de Paleontología y Estratigrafía, No. 1, Actas 2: 173-228. San Miguel de Tucumán.

Damborenea, S.E.; Manceñido, M.O. 1993. Piedra Pintada. *In* Léxico Estratigráfico de la Argentina, Volumen IX, Jurásico: 313 (Riccardi, A.C.; Damborenea, S. E.; editors). Asociación Geológica Argentina, Serie 'B' (Didáctica y Complementaria) No. 21: 313-316. Buenos. Aires.

Davidson, J.; De Silva, S. 2000. Composite volcanoes. *In* Encyclopedia of Volcanoes (Sigurdsson, H.; Houghton, B.; McNutt, S.R.; Rymer, H.; Stix, J.; editors). Academic Press: 663-682. San Diego.

D'Elia, L. 2008. Estratovolcanes en el Precuyano del sur de la Cuenca Neuquina: asociaciones de facies y unidades de acumulación en la Formación Sañicó. *In* Reunión Argentina de Sedimentología, No. 12. Actas: p. 65. Buenos Aires.

D'Elia, L. 2010. Application of the allostratigraphic approach to the study of volcano-sedimentary rift sequences: an example from the Jurassic of the Neuquén Basin, Argentina. *In* International Sedimentological Congress, No. 18, Digital abstracts. Mendoza.

D'Elia, L.; Franzese, J.R. 2005. Caracterización litológica y estructural de ignimbritas precuyanas en la sierra de Chacaico, Neuquén, con énfasis en su potencial petrolero. *In* Congreso de Exploración de Hidrocarburos, No. 6. Trabajos técnicos, Reservorios y desarrollo de reservas. Resúmenes de trabajos: 27. Edición en CD-ROM. Mar del Plata.

D'Elia, L.; Muravchik, M.; Franzese, J.R.; Bilmes, A. 2012. Syn-rift volcanism of the Neuquén Basin, Argentina: relationships with the Late Triassic-Early Jurassic evolution of the Andean margin. Andean Geology 39 (1): 106-132.

Fisher, R.V.; Schmincke, H-U. 1984. Pyroclastic rocks. Springer-Verlag: 472 p. New York.

Franzese, J.R.; Spalletti, L.A. 2001. Late Triassic-early Jurassic continental extension in southwestern Gondwana: tectonic segmentation and pre-break-up rifting. Journal of South American Earth Sciences 14: 257-270.

Franzese, J.R.; Veiga, G.D.; Muravchik, M.; Ancheta, D.; D'Elía, L. 2007. Estratigrafía de 'sin-rift' (Triásico Superior-Jurásico Inferior) de la Cuenca Neuquina en la sierra de Chacaico, Neuquén, Argentina. Revista Geológica de Chile 34 (1): 49-62.

Franzese, J.R.; Veiga, G.D.; Schwarz, E.; Gómez-Pérez, I. 2006. Tectonostratigraphic evolution of a Mesozoic graben border system: the Chachil depocentre, southern Neuquén Basin, Argentina. Journal of the Geological Society 163: 707-721.

Frenguelli, J. 1948. Estratigrafía y Edad del Llamado 'Retico' en la Argentina. Anales de la Sociedad Argentina de Estudios Geográficos GAEA 8: 159-309.

Galli, C.A. 1953. Acerca de una nueva interpretación de las formaciones rético-liásica de la Patagonia septentrional. Revista de la Asociación Geológica Argentina 8 (4): 220-235.

Galli, C.A. 1969. Descripción Geológica de la Hoja 38c, Piedra del Águila (provincias del Neuquén y Río Negro). Dirección Nacional de Geología y Minería, Boletín 111: 1-67. Buenos Aires.

Gawthorpe, R.L.; Jackson, C.A.L.; Young, M.; Sharp, I.R.; Moustafa, A.; Leppard, C.V. 2003. Normal fault growth, displacement localisation and the evolution of normal fault populations: the Hammam Faraun fault block, Suez Rift, Egypt. Journal of Structural Geology 25: 883-895.

Gawthorpe, R.L.; Leeder, M.R. 2000. Tectono-sedimentary evolution of active extensional basins. Basin Research 12: 195-218.

Giambiagi, L.; Bechis, F.; Barredo, S.; Tunik, M. 2008a. Cinemática de la apertura de los depocentros Atuel y Cara Cura - Reyes, Cuenca Neuquina: rift con múltiples sets de fallas. *In* Congreso de Exploración y Desarrollo de Hidrocarburos, No. 7, Trabajos Técnicos: 431-442. Mar del Plata.

Giambiagi, L.; Bechis, F.; Tunik, M.; Barredo, S. 2008b. Cuencas de rift con múltiples sets de fallas: caso de es-

tudio del sector septentrional de la Cuenca Neuquina. *In* Congreso Geológico Argentino, No.17, Actas 2: 767-768. San Salvador de Jujuy.

Giambiagi, L.; Bechis, F.; Lanés, S.; Tunik, M.; García, V.; Suriano, J.; Mescua, J. 2008c. Formación y evolución triásico-jurásica del depocentro Atuel, Cuenca Neuquina, provincia de Mendoza. Revista de la Asociación Geológica Argentina 63 (4): 520-533.

Gifkins, C.C.; Allen, R.L.; McPhie, J. 2005. Apparent welding textures in altered pumice-rich rocks. Journal of Volcanology and Geothermal Research 142 (1-2): 29-47.

Gulisano, C. 1981. El ciclo cuyano en el norte de Neuquén y sur de Mendoza. *In* Congreso Geológico Argentino, No. 8, Actas 3: 579-592. San Luis.

Gulisano, C.A. 1993. Precuyano. *In* Léxico Estratigráfico de la Argentina, Volumen IX, Jurásico: 334 (Riccardi, A.C.; Damborenea, S.E.; editors). Asociación Geológica Argentina. Serie 'B' (Didáctica y Complementaria) No. 21: 334-335. Buenos. Aires.

Gulisano, C.A.; Gutiérrez Pleimling, A.R. 1994. The Jurassic of the Neuquén Basin. Part (a) Neuquén Province. Asociación Geológica Argentina, Serie D-2: 1-111.

Gulisano, C.A.; Gutiérrez Pleimling, A.R.; Digregorio, R.E. 1984. Esquema estratigráfico de la secuencia jurásica del oeste de la provincia del Neuquén. *In* Congreso Geológico Argentino, No. 9, Actas I: 236-259. San Carlos de Bariloche.

Gulisano, C.; Pando, G.A. 1981. Estratigrafía y facies de los depósitos jurásicos entre Piedra del Águila y Sañicó, Departamento Collón Curá, Provincia del Neuquén. *In* Congreso Geológico Argentino, No. 8, Actas 3: 553-577. San Luis.

Herbst, R. 1966. Revisión de la flora liásica de Piedra Pintada, provincia del Neuquén, Argentina. Revista del Museo de La Plata (nueva serie) Paleontología 5 (30): 27-53.

Howell, J.A.; Schwarz, E.; Spalletti, L.A.; Veiga, G.D. 2005. The Neuquén Basin: an overview. *In* The Neuquén Basin, Argentina: A Case Study in Sequence Stratigraphy and Basin Dynamics (Veiga, G.D.; Spalletti, L.A.; Howell, J.A.; Schwarz, E.; editors). Geological Society, London, Special Publications 252: 1-14.

Jackson, C.A.L.; Gawthorpe, R.L.; Carr, I.D.; Sharp, I.R. 2005. Normal faulting as a control on the stratigraphic development of shallow marine syn-rift sequences: the Nukhul and Lower Rudeis Formations, Hammam Faraun fault blocks, Suez Rift, Egypt. Sedimentology 52: 313-338.

Kilburn, C.R.F. 2000. Lava flows and flow fields. *In* Encyclopedia of Volcanoes (Sigurdsson, H.; Houghton, B.; McNutt, S.R.; Rymer, H.; Stix, J.; editors). Academic Press: 307-320. San Diego.

Kokelaar, P.; Raine, P.; Branney, M.J. 2007. Incursion of a large-volume, spatter-bearing pyroclastic density current into a caldera lake: Pavey Ark ignimbrite, Scafell caldera, England. Bulletin of Volcanology 70: 23-54.

Lambert, L.R.; Galli, C.A. 1950. Observaciones geológicas en la región situada entre Piedra del Águila y Paso Flores (Neuquén). Revista de la Asociación Geológica Argentina 5 (4): 227-232.

Leanza, H.A. 1990. Estratigrafía del Paleozoico y Mesozoico anterior a los movimientos intermálmicos en la Comarca del Cerro Chachil, Provincia del Neuquén. Revista de la Asociación Geológica Argentina 45 (3-4): 272-299.

Legarreta, L.; Uliana, M.A. 1996. The Jurassic succession in west-central Argentina: stratal pattern, sequences and paleogeographic evolution. Palaeogeography, Palaeoclimatology and Palaeoecology 120: 303-330

Lipman, P.W. 2000. Calderas. *In* Encyclopedia of Volcanoes (Sigurdsson, H.; Houghton, B.; McNutt, S.R.; Rymer, H.; Stix, J.; editors). Academic Press: 643-662. San Diego.

Llambías, E.J.; Leanza, H.A.; Carbone, O. 2007. Evolución tectono-magmática durante el Pérmico al Jurásico temprano en la Cordillera del Viento (37°05'S-37°15'S): Nuevas evidencias geológicas y geoquímicas del inicio de la Cuenca Neuquina. Revista de la Asociación Geológica Argentina 62 (2): 217-235.

Marsh, B.D. 2000. Magma chambers. Composite volcanoes. *In* Encyclopedia of Volcanoes (Sigurdsson, H.; Houghton, B.; McNutt, S.R.; Rymer, H.; Stix, J.; editors). Academic Press: 191-206. San Diego.

McArthur, A.M.; Cas, R.A.F.; Orton, G.J. 1998. Distribution and significance of crystalline, perlitic and vesicular textures in the Ordovician Garth Tuff (Wales). Bulletin of Volcanology 60: 260-285.

McPhie, J.; Doyle, M.; Allen, R. 1993. Volcanic Textures: a guide to the interpretation of textures in volcanic rocks. CODES-University of Tasmania: 198 p. Hobart.

Miall, A.D. 1978. Fluvial Sedimentology. Canadian Society of Petroleum Geologists Memoir 5: 859 p. Calgary.

Miall, A.D. 2006. The Geology of Fluvial Deposits. Springer: 582 p. Berlin.

Moore, I.; Kokelaar, P. 1997. Tectonic influences in piecemeal caldera collapse at Glencoe Volcano, Scotland. Journal of the Geological Society 154: 765-768.

Moore, I.; Kokelaar, P. 1998. Tectonically controlled piecemeal caldera collapse: A case study of Glencoe volcano, Scotland. Geological Society of America Bulletin 110: 1448-1466.

Morabito, E.G.; Götze, H-J; Ramos, V.A. 2011. Tertiary tectonics of the Patagonian Andes retro-arc area between 38°15' and 40°S latitude. Tectonophysics 499: 1-21.

Morel, E.M.; Ganuza, D.G. 2002. Formación Paso Flores. *In* Léxico Estratigráfico de la Argentina 8. Triásico (Stipanicic, P.N.; Marsiscano, C.A.; editors). Asociación Geológica Argentina, Serie B (Didáctica y Complementaria) No. 26: 208-209. Buenos Aires.

Morley, C.K. 1995. Developments in the structural geology of rifts over the last decade and their impact on hydrocarbon exploration. *In* Hydrocarbon Habitat in rift basins (Lambiase, J.J.; editor). Geological Society Special Publication 80: 1-32.

Morley, C.K. 1999a. Basin Evolution Trends in East Africa. *In* Geoscience of rift systems-Evolution of East Africa (Morley, C.K.; editor). American Association of Petroleum Geologists (AAPG) Studies in Geology 44: 131-150.

Morley, C.K. 1999b. How successful are analogue models in addressing the influence of pre-existing fabrics on rift structure? Journal of Structural Geology 21: 1267-1274.

Morley, C.K.; Haranya, C.; Phoosongsee, W.; Pongwapee, S.; Kornsawan, A.; Wanganan, N. 2004. Activation of rift oblique and rift parallel pre-existing fabrics during extension and their effect on deformation style: examples from the rifts of Thailand. Journal of Structural Geology 26: 1803-1829.

Moustafa, A.R. 2002. Controls on the geometry of transfer zones in the Suez rift and northwest Red Sea: implications for the structural geometry of rift systems. American Association of Petroleum Geologists (AAPG) Bulletin 86 (6): 979-1002.

Mpodozis, C.; Ramos, V.A. 2008. Tectónica Jurásica en Argentina y Chile: extensión, subducción oblicua, rifting, deriva y colisiones. Revista de la Asociación Geológica Argentina 63 (4): 481-497.

Muravchik, M.; D'Elia, L.; Bilmes, A.; Franzese, J.R. 2008. Caracterización de los depocentros de rift (Ciclo Precuyano) aflorantes en el sector sudoccidental de la Cuenca Neuquina, Argentina. *In* Congreso de Exploración y Desarrollo de Hidrocarburos, No. 7, Trabajos Técnicos: 457-470. Mar del Plata.

Muravchik, M.; D'Elia, L. 2010. Sedimentary environments in volcanic rift depocentres, Neuquén Basin, Argentina. *In* International Sedimentological Congress, No. 18, Digital abstracts. Mendoza.

Muravchik, M.; D'Elia, L.; Bilmes, A.; Franzese, J.R. 2011. Syn-eruptive/inter-eruptive relations in the syn-rift deposits of the Precuyano Cycle, Sierra de Chacaico, Neuquén Basin, Argentina. Sedimentary Geology 238 (1-2): 132-144.

Muravchik, M.; Franzese, J.R. 2005. Carbonatos lacustres someros en las facies volcaniclásticas del Precuyano de la sierra de Chacaico, Neuquén. *In* Congreso Geológico Argentino, No. 16, Actas 3: 111-116. La Plata.

Németh, K.; Ulrike, M. 2007. Practical Volcanology. Lecture notes for understanding volcanic rocks from field-based studies. Occasional Papers of the Geological Institute of Hungary 27: 221 p. Budapest.

Palmer, B.A.; Purves, A.M.; Donoghue, S.L. 1993. Controls on accumulation of a volcaniclastic fan, Ruapehu composite volcano, New Zealand. Bulletin of Volcanology 55: 176-189.

Pángaro, F.; Corbera, R.; Carbone, O.; Hinterwimmer, G. 2002. Los reservorios del Precuyano. *In* Rocas Reservorio de las Cuencas Productivas Argentinas (Schiuma, M.; Hinterwimmer, G.; Vergani, G.D.; editores). Instituto Argentino del Petróleo y del Gas: 229-254. Buenos Aires.

Pángaro, F.; Pereira, D.M.; Micucci, E. 2009. El sinrift de la dorsal de Huincul, Cuenca Neuquina: evolución y control sobre la estratigrafía y estructura del área. Revista de la Asociación Geológica Argentina 65 (2): 265-277.

Petrinovic, I.A.; Martí, J.; Aguirre-Díaz, G.J.; Guzmán, S.; Geyer, A.; Salado Paz, N. 2010. The Cerro Aguas Calientes caldera, NW Argentina: an example of a tectonically controlled, polygenetic collapse caldera, and its regional significance. Journal of Volcanology and Geothermal Research 194 (1-3): 15-26.

Price, R.C.; Gamble, J.A.; Smith, I.E.M.; Stewartd, R.B.; Eggins, S.; Wright, I.C. 2005. An integrated model for the temporal evolution of andesites and rhyolites and crustal development in New Zealand's North Island. Journal of Volcanology and Geothermal Research 140: 1-24.

Ramos, V.A. 2009. Anatomy and global context of the Andes: main geologic features and the Andean orogenic cycle. *In* Backbone of the Americas: Shallow Subduction, Plateau Uplift, and Ridge and Terrane

Collision (Kay, S.M.; Ramos, V.A.; Dickinson, W.R.; editors). Geological Society of America Memoir 204: 31-65.

Ramos, V.A.; Folguera, A. 2005. Tectonic evolution of the Andes of Neuquén: constraints derived from the magmatic arc and foreland deformation. *In* The Neuquén Basin, Argentina: A Case Study in Sequence Stratigraphy and Basin Dynamics (Veiga, G.D.; Spalletti, L.A.; Howell, J.A.; Schwarz, E.; editors). Geological Society, Special Publications: 15-35. London.

Ramos, V.; Kay, S. 1991. Triassic rifting and associated basalts in the Cuyo basin, central Argentina. *In* Andean Magmatism and its Tectonic Setting (Harmon, R.S.; Rapela, C.W. editors). Geological Society of America, Special Paper 265: 79-91. Boulder.

Reading, H.G.; Collinson, J.D. 2002. Clastic coasts. *In* Sedimentary Environments: Processes, Facies and Stratigraphy (Reading, H.G.; editor). Blackwell Science: 154-231. Oxford.

Reubi, O.; Hernández, J. 2000. Volcanic debris avalanche deposits of the upper Maronne valley (Cantal Volcano, France): evidence for contrasted formation and transport mechanisms. Journal of Volcanology and Geothermal Research 102: 271-286.

Riccardi, A.C.; Gulisano, C.A. 1990. Unidades limitadas por discontinuidades. Su aplicación al Jurásico andino. Revista de la Asociación Geológica Argentina 45 (3-4): 346-364.

Riding, R.; 2000. Microbial carbonates: the geological record of calcified bacterial-algal mats and biofilms. Sedimentology 47 (1): 179-214.

Rohais, S.; Eschard, R.; Guillocheau, F. 2008. Depositional model and stratigraphic architecture of rift climax Gilbert-type fan deltas (Gulf of Corinth, Greece). Sedimentary Geology 210: 132-145.

Rowland, J.V.; Wilson, C.J.N.; Gravley, D.M. 2010. Spatial and temporal variations in magma-assisted rifting, Taupo Volcanic Zone, New Zealand. Journal of Volcanology and Geothermal Research 190: 89-108.

Schiuma, M.; Llambías, E.J. 2008. New ages and chemical analysis on Lower Jurassic volcanism close to the Huincul High, Neuquén. Revista de la Asociación Geológica Argentina 63 (4): 644-652.

Schlische, R.W. 1991. Half-graben basin filling models: new constraints on continental extensional basin development. Basin Research 3: 123-141.

Schlische, R.W. 1992. Structural and stratigraphic development of the Newark extensional basin, eastern North America: evidence for the growth of the basin and its bounding structures. Geological Society of America Bulletin 104: 1246-1263.

Schlische, R.W.; Anders, M.H. 1996. Stratigraphic effects and tectonic implications of the growth of normal faults and extensional basins. Geological Society of America, Special paper 303: 183-203.

Schneider, J.; Fisher, R.V. 1998. Transport and emplacement mechanisms of large volcanic debris avalanches: evidence from the northwest sector of Cantal Volcano (France). Journal of Volcanology and Geothermal Research 83: 141-165.

Sesana, F. 1968. Rasgos petrológicos de la comarca de Río Chico, Río Negro. *In* Jornadas Geológicas Argentinas, No. 3, Actas 3: 99-107. Buenos Aires.

Shea, T.; van Wyk de Vries, B.; Pilato, M. 2008. Emplacement mechanisms of contrasting debris avalanches at Volcán Mombacho (Nicaragua), provided by structural and facies analysis. Bulletin of Volcanology 70 (8): 899-921.

Smith, G.A. 1986. Coarse-Grained Nonmarine Volcanoclastic Sediment-Terminology and Depositional Process. Geological Society of America Bulletin 97: 1-10.

Smith, G.A. 1987. The influence of explosive volcanism on fluvial sedimentation: the Deschutes Formation (Neogene) in Central Oregon. Journal of Sedimentary Petrology 57: 613-629.

Smith, G.A. 1991. Facies sequences and geometries in continental volcaniclastic sediments. *In* Sedimentation in Volcanic Settings (Fisher, R.V.; Smith, G.A.; editors). Society of Economic Paleontologists and Mineralogists, Special Publication: 45: 109-121. Tulsa.

Smith, G.A.; Lowe, D.R. 1991. Lahars: Volcano-hydrologic events and deposition in the debris flow-hyperconcentrated flow continuum. *In* Sedimentation in Volcanic Settings (Fisher, R.V.; Smith, G.A.; editors). Society of Economic Paleontologists and Mineralogists, Special Publication: 45: 59-70. Tulsa.

Spalletti, L.A.; Franzese, J.R.; Morel, E.; D'Elia, L.; Zúñiga, A.; Fanning C.M. 2010. Consideraciones acerca de la sedimentología, paleobotánica y geocronología de la Formación Piedra del Águila (Jurásico Inferior, Neuquén, República Argentina). Revista de la Asociación Geológica Argentina 66 (3): 305-313.

Spinks, K.D.; Acocella, V.; Cole, J.W.; Bassett, K.N. 2005. Structural control of volcanism and caldera development in the transtensional Taupo Volcanic Zone, New Zealand. Journal of Volcanology and Geothermal Research 144: 7-22.

Stewart, A.L.; McPhie, J. 2003. Internal structure and emplacement of an Upper Pliocene dacite cryptodome, Milos Island, Greece. Journal of Volcanology and Geothermal Research 124: 129-148.

Stewart, A.L.; McPhie, J. 2006. Facies architecture and Late Pliocene-Pleistocene evolution of a felsic volcanic island, Milos, Greece. Bulletin of Vulcanology 68: 703-726.

Stipanicic, P.N. 1967. Consideraciones sobre las edades de algunas fases magmáticas del Neopaleozoico y Mesozoico. Revista de la Asociación Geológica Argentina 22 (2): 101-133.

Stipanicic, P.N. 1969. El avance de los conocimientos del Jurásico argentino a partir del esquema de Groeber. Revista de la Asociación Geológica Argentina 24 (4): 367-388.

Stipanicic, P.N.; Rodrigo, F.; Baulies, O.L.; Martínez, C.G. 1968. Las formaciones presenonianas en el denominado Macizo Nordpatagónico y regiones adyacentes. Revista de la Asociación Geológica Argentina 23 (2): 67-98.

Talbot, M.R.; Allen, P.A. 2002. Lakes. *In* Sedimentary environments: Processes, Facies and Stratigraphy (Reading, H.G.; editor). Blackwell Science: 83-124. Oxford.

Varela, R.; Basei, M.A.S.; Cingolani, C.A.; Siga Jr., O.; Passarelli, C.R. 2005. El basamento cristalino de los Andes norpatagónicos en Argentina: geocronología e interpretación tectónica. Revista Geológica de Chile 32 (2): 167-187.

Varela, R.; Dalla Salda, L.; Cingolani, C.; Gómez, V. 1991. Estructura, petrología y geocronología del basamento de la región del Río Limay del Río Negro y Neuquén, Argentina. Revista Geológica de Chile, 18 (2): 147-163.

Vergani, G.D.; Tankard, A.J.; Belotti, H.J.; Weisink, H.J. 1995. Tectonic evolution and paleogeography of the Neuquén basin, Argentina. *In* Petroleum basins of South America (Tankard, A.J.; Suárez, S.R.; Welsink, H.J.; editors). American Association of Petroleum Geologists (AAPG) Memoir 62: 383-402.

Volkheimer, W. 1964. Estratigrafía de la zona extra-andina del departamento de Cushamen (Chubut) entre los paralelos 42º y 42º30' y los meridianos 70º y 71º. Revista de la Asociación Geológica Argentina 19 (2): 85-107.

Walker, R.G. 2006. Facies models revisited. *In* Facies Models Revisited (Posamentier, H.W.; Walker, R.G.; editors). Society for Sedimentary Geology (SEPM) Special Publication 84: 1-17. Tulsa.

Wilson, M. 1989. Igneous Petrogenesis: A Global Tectonic Approach. Chapman and Hall: 446 p. Londres.

Young, M.J.; Gawthorpe, R.L.; Sharp, I.R. 2003. Normal fault growth and early syn-rift sedimentology and sequence stratigraphy: Thal Fault, Suez Rift, Egypt. Basin Research 15: 479-502.

Zancheta, G.; Sulpicio, R.; Di Vito, M.A. 2004. The role of volcanic activity and climate in alluvial fan growth at volcanic areas: an example from southern Campania (Italy). Sedimentary Geology 168 (3-4): 249-280.

Manuscript received: February 24, 2011; revised/accepted: August 08, 2011; available online: August 18, 2011.